1972

Hydraulic performance of pennsylvania highway drainage inlets (Type J, Type 4-Ft. Special, and Type 6-Ft. Special), November 1972

Peter Yee

Walter H. Graf

Arthur W. Brune

COMMONWEALTH OF PENNSYLVANIA
DEPARTMENT OF TRANSPORTATION

BUREAU OF MATERIALS, TESTING AND RESEARCH
RESEARCH REPORT

RESEARCH PROJECT 68-31

DEVELOPMENT OF IMPROVED DRAINAGE INLETS

HYDRAULIC PERFORMANCE OF PENNSYLVANIA HIGHWAY DRAINAGE INLETS INSTALLED IN PAVED CHANNELS

by

Peter P. Yee

Walter H. Graf

Arthur W. Brune

LEHIGH UNIVERSITY

Office of Research

Fritz Engineering Laboratory Report No. 364.3

TECHNICAL REPORT STANDARD TITLE PAGE

1. Report No.	2. Government Accession No.	3. Recipient's Catalog No.

4. Title and Subtitle	5. Report Date
HYDRAULIC PERFORMANCE OF PENNSYLVANIA HIGHWAY DRAINAGE INLETS INSTALLED IN PAVED CHANNELS	November 1972
	6. Performing Organization Code
7. Author(s) Peter P. Yee, Walter H. Graf, and Arthur W. Brune	8. Performing Organization Report No. Fritz Engineering Laboratory Report 364.3
9. Performing Organization Name and Address Lehigh University Department of Civil Engineering Bethlehem, Pennsylvania 18015	10. Work Unit No.
	11. Contract or Grant No. PennDOT 68-31
	13. Type of Report and Period Covered Interim Report
12. Sponsoring Agency Name and Address Commonwealth of Pennsylvania Department of Transportation P. O. Box 2926 Harrisburg, Pennsylvania 17120	14. Sponsoring Agency Code

15. Supplementary Notes

Prepared in cooperation with the U. S. Department of Transportation, Federal Highway Administration.
From the study "Development of Improved Drainage Inlets."

16. Abstract

The capacities of three different standard inlets gratings installed in paved channels by the Pennsylvania Department of Transportation were determined in a paved drainage channel equipped with adjustable slopes. The longitudinal slope ranged from 0.5% to 8%; one side slope ranged from 48:1 to 12:1; and the other slope was at an inclination of either 3:1 or 1/8:1. The drainage inlets studied were (1) Type J Inlet, (2) Type 4-Ft. Special Inlet, and (3) Type 6-Ft. Special Inlet.

Model inlets were built to half the scale of the actual inlets. Each inlet was tested under a variety of channel configurations and with a certain range of channel flow rates. The capacity of an inlet was determined by actual measurements, and thus the efficiency of each inlet was obtained. A series of curves, relating efficiency to capacity for an inlet, are presented in the study. The curves show that as more water flows in the channel toward an inlet the efficiency of the inlet decreases.

The knowledge obtained from this investigation provides information that is more adequate to the designer in determining the spacing of highway drainage inlets than the information presently available.

17. Key Words	18. Distribution Statement
Capacity of inlets, Channels Drainage Design Capacity, Drainage, Efficiency, Gratings, Highway Drainage, Inlets, Model Tests, Models, Runnoff, Water.	

19. Security Classif. (of this report)	20. Security Classif. (of this page)	21. No. of Pages	22. Price
Unclassified	Unclassified	82	

Form DOT F 1700.7 (8-69)

COMMONWEALTH OF PENNSYLVANIA

Department of Transportation

Bureau of Materials, Testing and Research

Leo D. Sandvig - Director
Wade L. Gramling - Research Engineer
Kenneth L. Heilman - Research Coordinator

PennDOT Research Project 68-31
Development of Improved Drainage Inlets

HYDRAULIC PERFORMANCE OF PENNSYLVANIA HIGHWAY DRAINAGE INLETS INSTALLED IN PAVED CHANNELS

(Type J, Type 4-Ft Special, and Type 6-Ft Special)

by

Peter P. Yee
Walter H. Graf
Arthur W. Brune

This report was prepared in cooperation with the Pennsylvania Department of Transportation and the United States Department of Transportation, Federal Highway Administration.

LEHIGH UNIVERSITY

Office of Research

Bethlehem, Pennsylvania

November 1972

Fritz Engineering Laboratory Report No. 364.3

ABSTRACT

An experimental investigation of the performances of some highway drainage inlets is presented. The purpose of this study was to provide information to aid in the design of spacing highway drainage inlets. The channel considered was triangular in cross-section with one side having slopes ranging from 48:1 to 12:1. The other side or back slope had a slope of either 1/8:1 or 3:1.

The drainage inlets studied were (1) Type J Inlet, (2) 4-Ft Special Inlet, and (3) 6-Ft Special Inlet. They are standard inlets used by the Pennsylvania Department of Transportation and are customarily installed in paved channels.

Model inlets were built to half the scale of actual inlets. Each inlet was tested under a variety of channel configurations and with a certain range of channel flow rates. The capacity of an inlet was determined by actual measurements, and thus the efficiency of an inlet was obtained.

A series of curves, relating efficiency to capacity for an inlet, are presented in the study. The curves show that as more water flows in the channel toward an inlet the efficiency of the inlet decreases. The knowledge obtained from this investigation provides information that is more adequate to the designer in determining the spacing of highway drainage inlets than the information presently available.

TABLE OF CONTENTS

TABLE OF CONTENTS (continued)

LIST OF FIGURES

LIST OF TABLES

LIST OF RECURRING SYMBOLS

B - width of water surface, ft

D - depth of channel, ft

F - force, lb

Fr - Froude number

g - gravitational acceleration, ft/sec^2

ΔH - pressure-head drop across orifice, ft

L - length, ft

ℓ - characteristic length, ft

M - mass, $lb\text{-}sec^2/ft$

n - Manning's roughness coefficient, $ft^{1/6}$

Q - flow rate (discharge), ft^3/sec

Q_1 - channel flow rate, ft^3/sec

Q_2 - intercepted flow rate, ft^3/sec

Q_3 - carryover flow rate, ft^3/sec

Q_4 - spillage over the divisor, ft^3/sec

Re - Reynolds number

R_h - hydraulic radius, ft

T - time, sec

$\forall$ - volume, ft^3

v - velocity, ft/sec

η - efficiency, percent

ρ - density, $slug/ft^3$

ν - kinematic viscosity, ft^2/sec

Subscripts

m - model

p - prototype

r - ratio

1. INTRODUCTION

1.1 Background and Need for Investigation

Runoff from rainfall can flow from highways into storm drainage systems through the drainage inlets which are placed at intervals along the roadside. Not uncommonly any particular drainage inlet is unable to accept all the water that comes to it owing to the limited capacity of the inlet and to clogging of the inlet openings by debris. The inability of the inlet to accept all the oncoming water can produce or lead to some undesirable conditions, such as, (1) encroachment of water onto the roadway pavement, thus creating safety hazards, (2) seepage of water into the subbase section of the highway, thus increasing the pore-water pressure of the soil aggregates, which might lead to premature failure of the highway, and (3) flooding of a low-lying area if water can not be completely drained from the highway by successive inlets placed along the roadside.

Design and spacing of drainage inlets have been governed by several factors, such as, (1) the assumed capacity of an inlet based on past experience, (2) the structural strength of the inlet gratings, (3) the effect of the inlet on traffic, (4) the effect of the inlet on pedestrians, and (5) installation and maintenance. At present the true capacities of many existing inlets are still unknown. Designers commonly assume that an inlet has a certain capacity regardless of the channel configuration, and little attention is paid to the carryover at an inlet, carryover being the water that by-passes the drainage inlet. Obviously, the capacity of any drainage inlet must be thoroughly understood if the spacing of inlets is to be set forth on a basis sounder than the current one.

An analytical approach to finding the capacities of an inlet is almost impossible if one considers the numerous variables that are involved, such as the longitudinal slope of the channel, the swale slope, the back slope, and the roughness of the channel. The sizes of the inlet and the different patterns of openings further complicate the whole matter. An alternative solution to the problem is actually testing a drainage inlet. Although that procedure can be followed under some conditions, other conditions indicate using models which are smaller in size than the prototypes.

Investigations of the performances of drainage inlets have been conducted by many researchers; prominent among them are the studies by LARSON et al. (1949), GUILLOU (1959), researchers at JOHNS HOPKINS UNIVERSITY (1956 and 1967), and U S ARMY CORPS OF ENGINEERS (1964). An extensive literature survey was made by YÜCEL et al. (1969). Inasmuch as the studies mentioned dealt with specific inlets, the results of those studies can not very well be made applicable to other inlets owing to the differences present between many inlets.

1.2 Scope of Study

This study deals primarily with determining the capacities of inlets by means of actually testing models of inlets. Six standard drainage inlets used by the Pennsylvania Department of Transportation (see Section 3.1) will be tested in the laboratory under a variety of conditions. Three of the inlets are customarily installed in paved channels. They are (1) Type 4-Ft Special, (2) Type 6-Ft Special, and (3) Type J. (See Figures 3.1, 3.2, and 3.3). The remaining three inlets, (1) Type H, (2) Type 4-Ft, and (3) Type 6-Ft, are installed on grassed channels. This study deals exclusively with the three inlets that are installed in paved channels.

No attempt was made to alter the geometry or the installation of any inlet tested in order to produce an increase in capacity of the inlet. All inlets were modelled according to specifications, and they were tested under a number of channel conditions and with a certain range of channel flow rates.

All inlet models were built with a prototype : model length ratio of 2:1. The knowledge of model laws was used to correlate model parameters to prototype parameters. As a result curves are presented that relate the efficiency of an inlet to its capacity. By means of this information a more rational design of inlet spacing is possible on the part of the hydraulic engineer.

2. MODEL LAWS

2.1 General Remarks

The use of models in hydraulic research is popular and common. Commonly, investigators find that certain flow phenomena cannot be studied because either (a) analytical methods are inherently inadequate, that is, the existing equations of fluid mechanics cannot be made applicable, or (b) experimental data are insufficient. The justification for the use of models is an economic one. Although in a few exceptions the size of the models is made larger than the size of the prototypes, models are usually made smaller than the prototypes. Another justification for the use of models is that testing of models can be done more readily in the laboratory. The results of such tests might even be used to check or to compare analytical results.

The cost in employing models is usually higher than that of analytical investigations. If the latter is deemed adequate in studying certain flow phenomena, then the use of models is not recommended.

The main purpose in modeling is to correlate model behavior to prototype behavior by means of basic principles of similitude. Once a prototype:model scale ratio is known, a relatively simple detailed interpretation of model measurements can be made. These results in turn can be translated into different physical quantities, such as velocity or discharge, in the corresponding prototype.

Numerous references deal with model laws and modeling. Those found to be particularly useful in this study are STEVENS et al. (1942), MORRIS (1963), HENDERSON (1966), VENNARD (1966), and GRAF (1971).

In the present study of highway drainage inlets, a prototype:model (length) ratio of 2:1 is used. Several factors were considered in establishing this ratio, such as, (a) the space available for testing a model, (b) the maximal discharge available in the laboratory, (c) the cost of fabrication and operation of the model, and (d) the effect of surface tension.

2.2 Principles of Hydraulic Similitude

Hydraulic similitude is the basic tool for correlating physical quantities between the model and the prototype. It can also be applied in cases where the linear scale ratio for vertical dimensions is different from that for horizontal dimensions; such models are referred to as distorted models. However, no distortion in the scales is used in the present study.

In order to correlate flow phenomena between model and prototype, three types of similitudes are involved; they are, geometrical similitude, kinematic similitude, and dynamic similitude. If complete similarity is desired between model and prototype, all three of the above similitudes must be satisfied. Each of the three will be discussed briefly in the following.

2.2.1 Geometrical Similarity

Two objects are said to be geometrical similar provided the ratios of corresponding dimensions are equal. In the model and prototype of Fig. 2.1, for example,

$$\frac{L_p}{L_m} = \frac{D_p}{D_m} = L_R = \frac{\ell_p}{\ell_m} \qquad (1)$$

where L and D denote the length of inlet and any depth of water, respectively, and ℓ is a characteristic length. The subscripts, p and m, refer to prototype and model, respectively. L_R is the scale ratio.

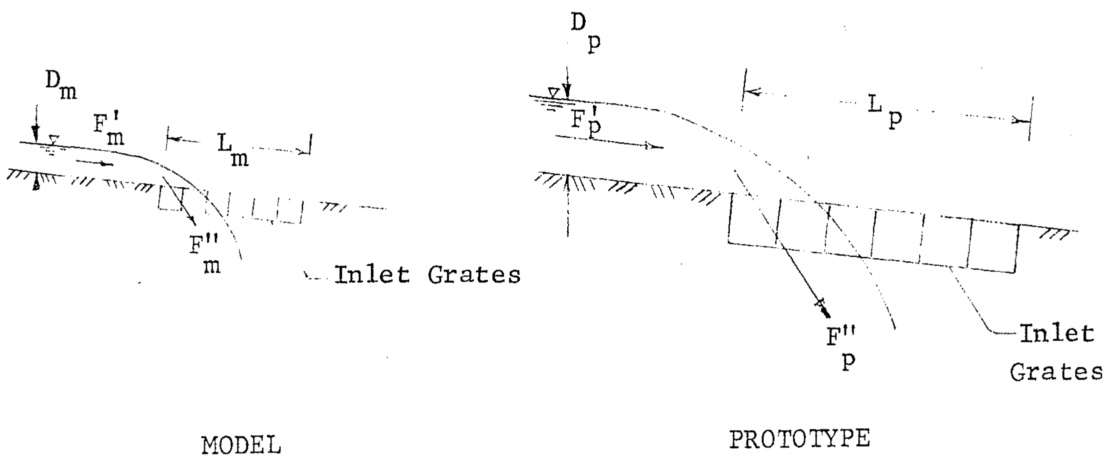

Fig. 2.1: Similitude of Highway Drainage Inlet

Corollaries of geometric similarity imply similarity of corresponding areas and volumes, such as:

$$\frac{A_p}{A_m} = L_R^2, \text{ and} \qquad (2)$$

$$\frac{\forall_p}{\forall_m} = L_R^3 , \qquad (3)$$

where A and ∀ denote area and volume, respectively.

2.2.2 Kinematic Similarity

Two flow phenomena are said to be kinematically similar provided (1) that the flow fields have the same shape, and (2) that the prototype:model ratios of corresponding velocities and accelerations are the same.

2.2.3 Dynamic Similarity

Dynamic similarity exists between model and prototype provided the prototype:model ratio of corresponding forces are the same. The force ratios shown in Fig. 2.1 may be written as:

$$\frac{F'_p}{F'_m} = \frac{F''_p}{F''_m} \qquad (4)$$

where F'_m and F''_m are two forces in the flow field of the model, and F'_p and F''_p are the corresponding forces in the corresponding flow field of the prototype. Owing to Newton's Law (Force = Mass x Acceleration), Eq. (4) requires that geometric and kinematic similarities be maintained between flow fields. In other words, dynamic similarity between prototype and model exists provided identical types of forces are parallel and have the same prototype:model ratio at all points in the corresponding flow fields.

2.3 Dimensionless Numbers

The forces which affect a flow field are those due to pressure, F_P, inertia, F_I, gravity, F_G, viscosity, F_V, elasticity, F_E, and surface tension, F_T. These forces are given by the following fundamental relationships:

$$F_P = (\Delta P)\ A = (\Delta P)\ \ell^2 \tag{5}$$

$$F_I = Ma = \rho\ell^3\ (\frac{v}{\ell})^2 = \rho v^2\ \ell^2 \tag{6}$$

$$F_G = Mg = \rho\ell^3\ g \tag{7}$$

$$F_V = \mu\ (\frac{dv}{dy})\ A = \mu\ (\frac{v}{\ell})\ \ell^3 = \mu\ v\ \ell \tag{8}$$

$$F_E = EA = E\ell^2 \tag{9}$$

$$F_T = \sigma\ell \tag{10}$$

where ΔP is a pressure difference; A is an area; ℓ is a characteristic length; ρ is density; M is a mass; a is acceleration; g is gravitational acceleration; μ is dynamic viscosity; E is the modulus of elasticity; and σ is the surface tension.

In the present study, the effects of elastic force, F_E, and of surface tension, F_T, can safely be neglected.

It has been stated previously that dynamic similarity implies similarity of forces; therefore, one may write:

$$\left(\frac{F_I}{F_P}\right)_p = \left(\frac{F_I}{F_P}\right)_m \; ; \; \left(\frac{\rho v^2}{\Delta P}\right)_p = \left(\frac{\rho v^2}{\Delta P}\right)_m \, , \tag{11}$$

$$\left(\frac{F_I}{F_V}\right)_p = \left(\frac{F_I}{F_V}\right)_m \; ; \; \left(\frac{v\rho\ell}{\mu}\right)_p = \left(\frac{v\rho\ell}{\mu}\right)_m \, , \text{ and} \tag{12}$$

$$\left(\frac{F_I}{F_G}\right)_p = \left(\frac{F_I}{F_G}\right)_m \; ; \; \left(\frac{v^2}{\ell g}\right)_p = \left(\frac{v^2}{\ell g}\right)_m \tag{13}$$

These force ratios which appear in Eq. (11) through (13) are better known as dimensionless numbers, and they are given the titles shown in Eq. (14) through (16).

Euler number: $$Eu = v\sqrt{\frac{\rho}{2\Delta P}} \tag{14}$$

Reynolds number: $$Re = \frac{v\ell\rho}{\mu} \tag{15}$$

Froude number: $$Fr = \frac{v}{\sqrt{\ell g}} \tag{16}$$

In this study Eq. (11) was of minor importance; therefore, dynamic similarity can be attained by satisfying the other two equations simultaneously.

However, it is almost impossible to have complete similarity between flow phenomena. In this study, as in most engineering problems, it is at times not necessary to satisfy all equations simulatenously. According to VENNARD (1966), some forces either (a) might not act, (b) might be of negligible magnitude, or (c) might oppose other forces in such a way that the effects of both are reduced. The predominant fluid forces that act in most hydraulic structures, such as, flow into a drainage inlet, are gravity, inertia, and viscous forces; the effects of surface tension and of elasticity are neglected owing to the large model and to compressibility being absent, respectively.

2.4 Froude Similitude

If one considers that flow at drainage inlets is primarily caused by gravitational forces, then the only criterion that needs to be satisfied is the Froude criterion, which can be stated as

$$Fr_p = Fr_m \text{ , or}$$

$$\left(\frac{v^2}{\ell g}\right)_p = \left(\frac{v^2}{\ell g}\right)_m \qquad (17)$$

where v is the mean flow velocity in fps, g is the acceleration of gravity in ft/sec^2, and ℓ is a characteristic length in ft.

Physical quantities for prototype and model can now be derived readily from the Froude relation. From Eq. (17) the prototype:model velocity ratio is obtained, such as

$$\frac{v_p^{\,2}}{v_m^{\,2}} = \frac{\ell_p g}{\ell_m g} \text{ ,} \qquad (18)$$

and inasmuch as gravity cannot be modeled, one obtains:

$$\frac{v_p}{v_m} = \left(\frac{\ell_p}{\ell_m}\right)^{1/2} \qquad (19)$$

With the scale ratio in the present study of $L_R = 2.0$, the velocity ratio becomes

$$\frac{v_p}{v_m} = 1.41 \tag{19a}$$

Furthermore, one can learn the flow rate in the prototype provided both the flow rate in the model and the prototype:model scale ratio are known. The discharge, Q, is given by the continuity equation; and with the knowledge of Eq. (2) and (19) one obtains:

$$\frac{Q_p}{Q_m} = \frac{A_p}{A_m} \cdot \frac{v_p}{v_m} = (L_R)^2 \ (L_R)^{1/2} = L_R^{5/2} , \tag{20}$$

where Q_p and Q_m denote the discharge in the prototype and in the model, respectively. With $L_R = 2.0$ in this study, Eq. (20) becomes

$$\frac{Q_p}{Q_m} = 5.66 \tag{20a}$$

Other characteristics of flow, such as area, volume, and time, can be readily obtained in a similar way. All of these ratios for a gravity or Froude model are shown in Table 2.1.

2.5 Manning Similitude

Although gravitational forces are very important in this problem, the effect of channel roughness should be investigated. In fact, the degree of roughness of the channel not only determines the

			Froude Similitude	Lehigh Univ. Scale	Manning Similitude	Lehigh Univ. Scale*
Physical Properties	Length	$\frac{\ell_p}{\ell_m}$	$\frac{\ell_p}{\ell_m}$	2.0	$\frac{\ell_p}{\ell_m}$	2.0
	Area	$\frac{A_p}{A_m}$	$\left(\frac{\ell_p}{\ell_m}\right)^2$	4.0	$\left(\frac{\ell_p}{\ell_m}\right)^2$	4.0
	Volume	$\frac{V_p}{V_m}$	$\left(\frac{\ell_p}{\ell_m}\right)^3$	8.0	$\left(\frac{\ell_p}{\ell_m}\right)^3$	8.0
Kinematic Properties	Time	$\frac{t_p}{t_m}$	$\left(\frac{\ell_p}{\ell_m}\right)^{1/2}$	1.41	$\left(\frac{\ell_p}{\ell_m}\right)^{1/3} \frac{n_p}{n_m}$	1.47
	Velocity	$\frac{v_p}{v_m}$	$\left(\frac{\ell_p}{\ell_m}\right)^{1/2}$	1.41	$\left(\frac{\ell_p}{\ell_m}\right)^{2/3} \frac{n_m}{n_p}$	1.36
	Discharge	$\frac{Q_p}{Q_m}$	$\left(\frac{\ell_p}{\ell_m}\right)^{5/2}$	5.66	$\left(\frac{\ell_p}{\ell_m}\right)^{8/3} \frac{n_m}{n_p}$	5.45

*$n_m = 0.012$, $n_p = 0.014$ (see Table 2.2)

Table 2.1: Model Scale for Froude Similitude and Manning Similitude

types of channel flow, but also affects the efficiency of the drainage inlet. Hence, it is desirable to consider both the forces of gravity and of friction or channel roughness. In order to do so, both the Froude model law and the Reynolds model law must be considered simultaneously. But it is impossible to satisfy both laws if the same fluid is to be used in both model and prototype. Other means of correlating prototype and model properties must be adopted.

An empirical relationship, such as the Manning formula, may be used as a friction criterion. The Manning formula is given as:

$$v = \frac{1.49\ R_h^{2/3}\ S^{1/2}}{n} \qquad (21)$$

where v is the mean velocity in fps, R_h is the hydraulic radius in ft and is equal to the cross-sectional area of water normal to the direction of flow divided by the wetted perimeter, n is the Manning coefficient of roughness, and S is the slope of energy grade line. If the flow is uniform, i.e., if a constant depth along the channel exists, then the slope of energy grade line and the slope of the water surface will be the same.

The friction criterion requires:

$$\left(\frac{R_h^{2/3}\ S^{1/2}}{v\,n}\right)_p = \left(\frac{R_h^{2/3}\ S^{1/2}}{v\,n}\right)_m \qquad (22)$$

Inasmuch as the model is not distorted, i.e., $S_p = S_n$, and if the hydraulic radius, R_h, is replaced by a suitable dimension, L, one obtains:

$$\left(\frac{L^{2/3}}{v\ n}\right)_p = \left(\frac{L^{2/3}}{v\ n}\right)_m . \qquad (23)$$

Because the discharge relationship between prototype and model is of prime interest, Eq. (23) can be rearranged to

$$\frac{Q_p}{Q_m} = \left(\frac{L_p}{L_m}\right)^{8/3} \frac{n_m}{n_p} \qquad (24)$$

This relationship and other flow characteristics for Manning similitude are shown in Table 2.1.

In order to evaluate Eq. (24), the roughnesses of the prototype and of the model, n_p and n_m, must be known. The Manning coefficient for the pavement was given by the Pennsylvania Department of Transportation as n = 0.014, which was in good agreement with the roughness cited in the literature, see CHOW (1959) and GRAF (1971). Plywood of 3/4-inch thickness has been used in the model in order to similate the paved surface of the prototype. The Manning coefficient of plywood had been determined from flume tests at Lehigh University and was found to be n = 0.012. This value is in close agreement with that as given by CHOW (1959). It has been decided that a value of n_p = 0.014 and n_m = 0.012 will be used. The Manning roughness study is summarized in Table 2.2.

Introducing the knowledge of the Manning's value ratio n_p/n_m = 0.014/0.012 and the length ratio of L_R = 2.0, Eq. (24) then becomes

$$\frac{Q_p}{Q_m} = 5.45 \qquad (24a)$$

n_{model}	$n_{prototype}$
Plywood	Concrete
n_m = 0.010 to 0.014 (CHOW (1959))	n_p = 0.011 to 0.015 (CHOW (1959))
n_m = 0.012 (Lehigh Univ.)	n_p = 0.014 (used by PennDOT)
n_m = 0.012 (used in this study)	n_p = 0.014 (used in this study)

Table 2.2: Manning Roughness Coefficients

The application of the Manning formula requires turbulent flow both in the model and in the prototype. Almost all open-channel flow found in nature is turbulent, whereas flow occurring in a similating model might very well not be turbulent. In order to ensure that turbulent flow does exist in the model, one should operate the model in such a way that a high Reynolds number, Re, is obtained.

In performing experiments in the model, it is then necessary to ascertain that turbulent flow does exist in it. The Reynolds number ratio from Eq. (15) is given as:

$$\frac{(Re)_p}{(Re)_m} = \frac{(vL)_p}{(vL)_m} \qquad (25)$$

By substituting Eq. (23) into Eq. (25), one obtains

$$\frac{(Re)_p}{(Re)_m} = 2.72 \qquad (25a)$$

A preliminary test was performed in the model, from which it was determined that turbulent flow does exist in the model.

2.6 Concluding Remarks

From observation of Table 2.1, the adoption of either one of the two similitudes - the Froude (gravity) and the Manning (roughness) similitudes - is a matter of choice. Gravity forces are more important, and Froude similitude has been selected for evaluating the results of this model.

3. EXPERIMENTAL INVESTIGATION

3.1 Inlets

Six different inlets are currently being installed along highways in Pennsylvania: these inlets are designated standards of the Pennsylvania Department of Transportation. They are (1) Type 4-Ft Special, (2) Type 6-Ft Special, (3) Type J, (4) Type H, (5) Type 4-Ft, and (6) Type 6-Ft. These inlets together with their specifications are summarized in Table 3.1. Each inlet differs from the other owing to the differences in installation as well as to the geometry of grate openings. However, Type 4-Ft Inlet and Type 4-Ft Special Inlet have the same grate openings; as is true of both Type 6-Ft Inlet and Type 6-Ft Special Inlet also.

All inlet gratings used in this study were made of wood. The first three inlets of Table 3.1 are installed on paved surfaces, whereas the last three are installed on channels that are usually covered with vegetation, specifically grass. Information pertaining to the two different surface roughnesses is shown in Table 2.2 and in Section 2.5. As a matter of convenience, it was decided that all those inlets installed on paved surfaces were to be tested first; Table 3.2 lists various channel conditions under which the first three inlets were to be tested.

3.1.1 Type 4-Ft Special and Type 6-FT Special Inlets

Figures 3.1(a) and 3.1(b) show the geometry of the gratings for the Type 4-FT Special Inlet and Type 6-Ft Special Inlet, respectively. The wooden frames of these inlet gratings were $2\frac{1}{2}$-inches

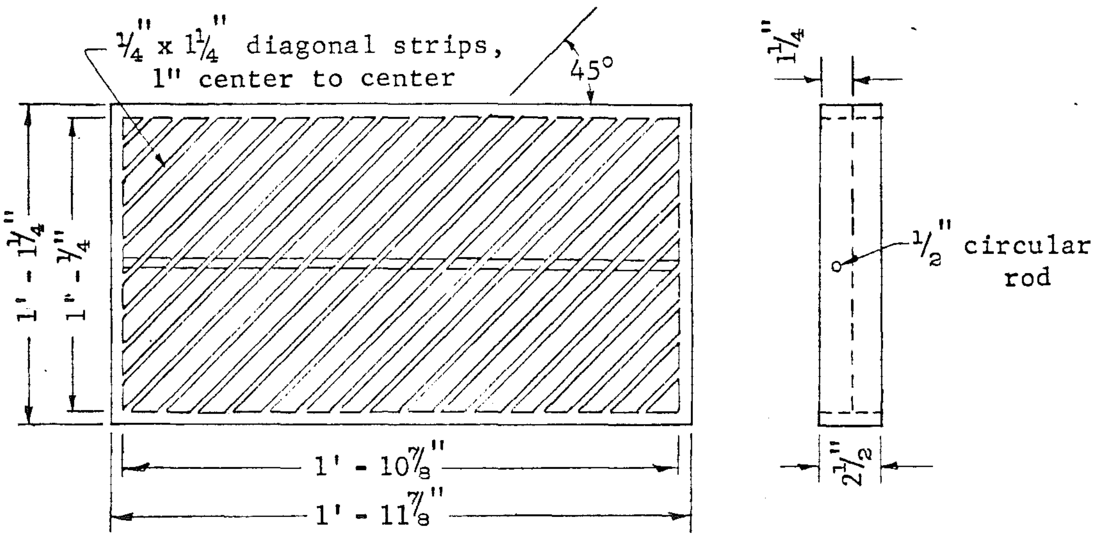

(a) Type 4-Ft Special Inlet

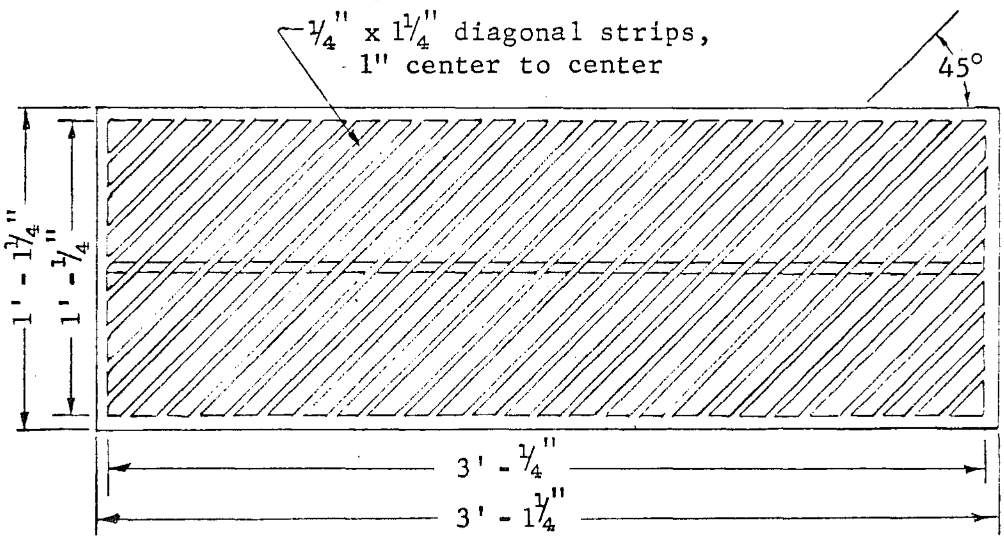

(b) Type 6-Ft Special Inlet

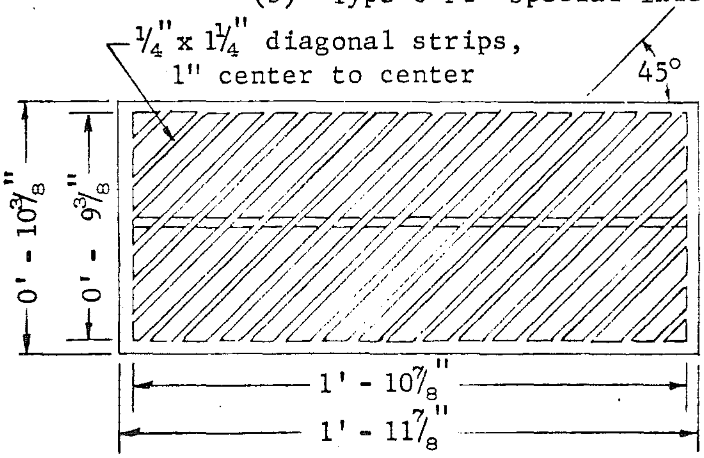

NOTE: All gratings are of the same height.

(c) Type J Inlet

Fig. 3.1 Model Inlet Grates

Inlet	Swale	Back Slope	Origin*
Type 4-Ft Special	Paved Area	Paved Area	(a)
Type 6-Ft Special	Paved Area	Paved Area	(a)
Type J	Paved Area	Paved Area	(b)
Type H	Grassed Area	Grassed Area	(c)
Type 4-Ft	Grassed Area	Grassed Area	(a)
Type 6-Ft	Grassed Area	Grassed Area	(a)

*Standard Drawings, Pennsylvania Department of Transportation.

(a) S.I. 4&6, Rev. Nov. 1, 1961 (RC-34, Dec. 1, 1971)

(b) Misc. Inlets, Type H and Type J Inlets, Approved May 8, 1968 (RC-35, Dec. 1, 1971)
SD-13, Type B Divisor, Approved May 13, 1966(RC-65, Dec. 1, 1971)

(c) Misc. Inlets, Type H and Type J Inlets, Approved May 8, 1968 (RC-35, Dec. 1, 1971)
Grating: (1) Standard Drawing: Misc. Inlets-Supplemental Sheet A.
(2) Longitudinal Bars, at 3-inch centers, suggested design.
(3) Diagonal Bars, at 3-inch centers, suggested design.

Table 3.1 Standard Inlets

deep by the model scale, rather than $1\frac{1}{2}$ inches as required for the purpose of rigidity. This change in depth of frames was considered to have no effect on water flowing through the gratings. Figure 3.2 shows the installation of the 4-Ft Special Inlet and the 6-Ft Special Inlet. The surface of the grating was flush with the surface of the plywood which simulated the pavement. Plywood of $\frac{3}{4}$-inch thickness and 8 inches in height was used to represent the curb that had a slope of 1/8:1. The hood which connected the curb opening and the vertical wall was made of 20-gauge galvanized steel.

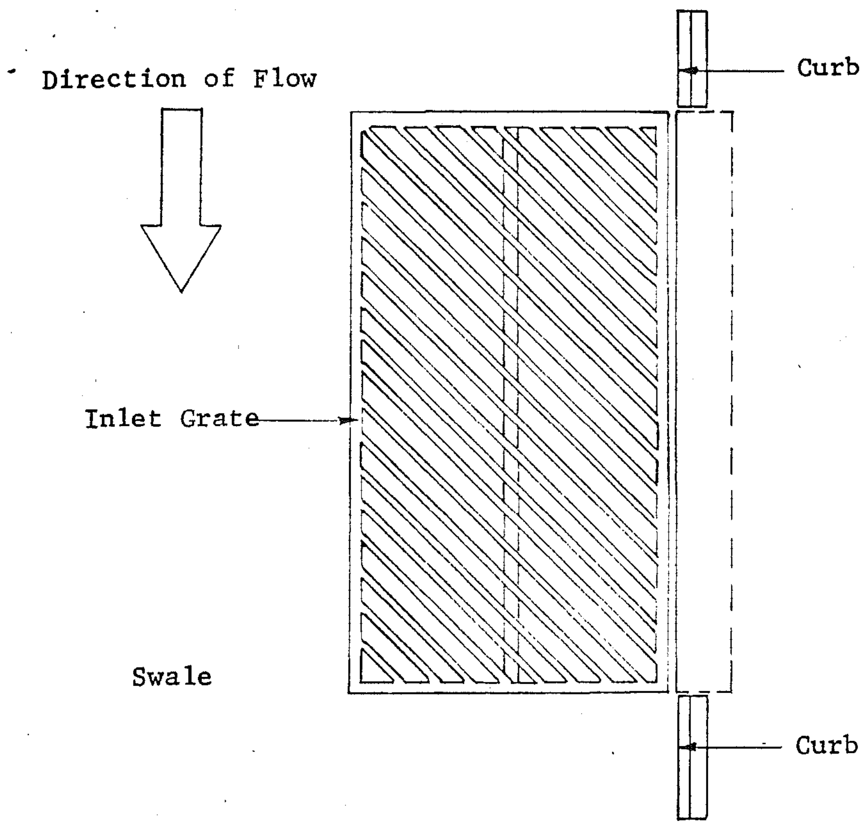

(a) Plan View

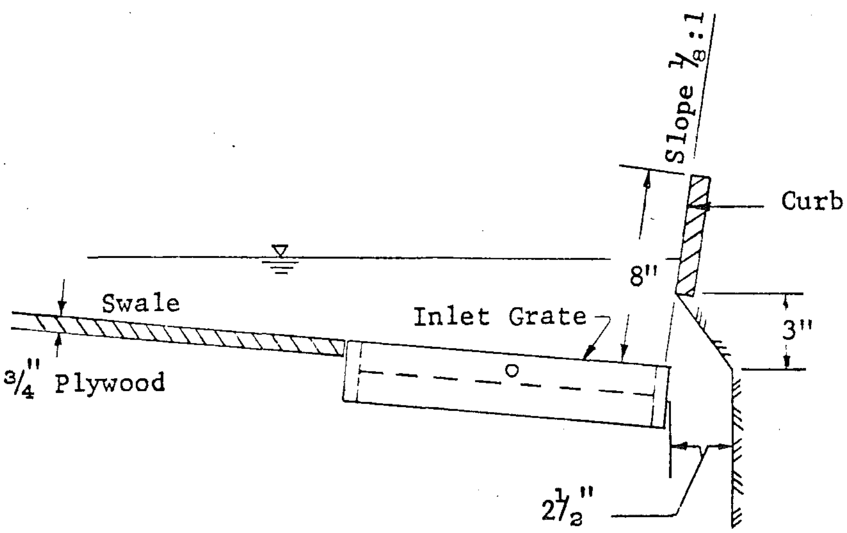

(b) Elevation View

Fig. 3.2 Installation for Type 4-Ft Special Inlet and Type 6-Ft Special Inlet

Inlet	Swale	Back Slope	Longitudinal Slope
Type 4-Ft Special	48:1,24:1, 16:1,12:1	1/8:1	0.5% , 2%, 4%, 8%
Type 6-Ft Special	48:1,24:1, 16:1,12:1	1/8:1	0.5% , 2%, 4%, 8%
Type J	48:1,24:1, 16:1,12:1	3:1	0.5% , 2%, 4%, 8%

Table 3.2 Order of Testing

3.1.2 Type J Inlet

Figure 3.1(c) shows the geometry of the grating for the Type J Inlet, and Fig. 3.3 shows its installation. The grating was flush with the plywood which simulated the pavement. The dimensions of the concrete divisor were taken from 'Type B Divisor' as appearing in the Pennsylvania Department of Transportation Standard Drawing: Concrete Mountable Curbs, Type A and B. Inasmuch as the water depth in the channel of the model did not exceed the height of the divisor at maximum channel discharge, only the half slope of the divisor adjacent to the flow was installed. The entire divisor was made of 20-gauge galvanized steel. The surface of the divisor was kept at a slope of 3:1 regardless of the swale slope. No scoring was made on this type divisor because lines of scoring are no longer made on this type of divisor as used on highways. The vertical wall along the inlet grating was 6 inches high and was made of 1/8-inch steel plate.

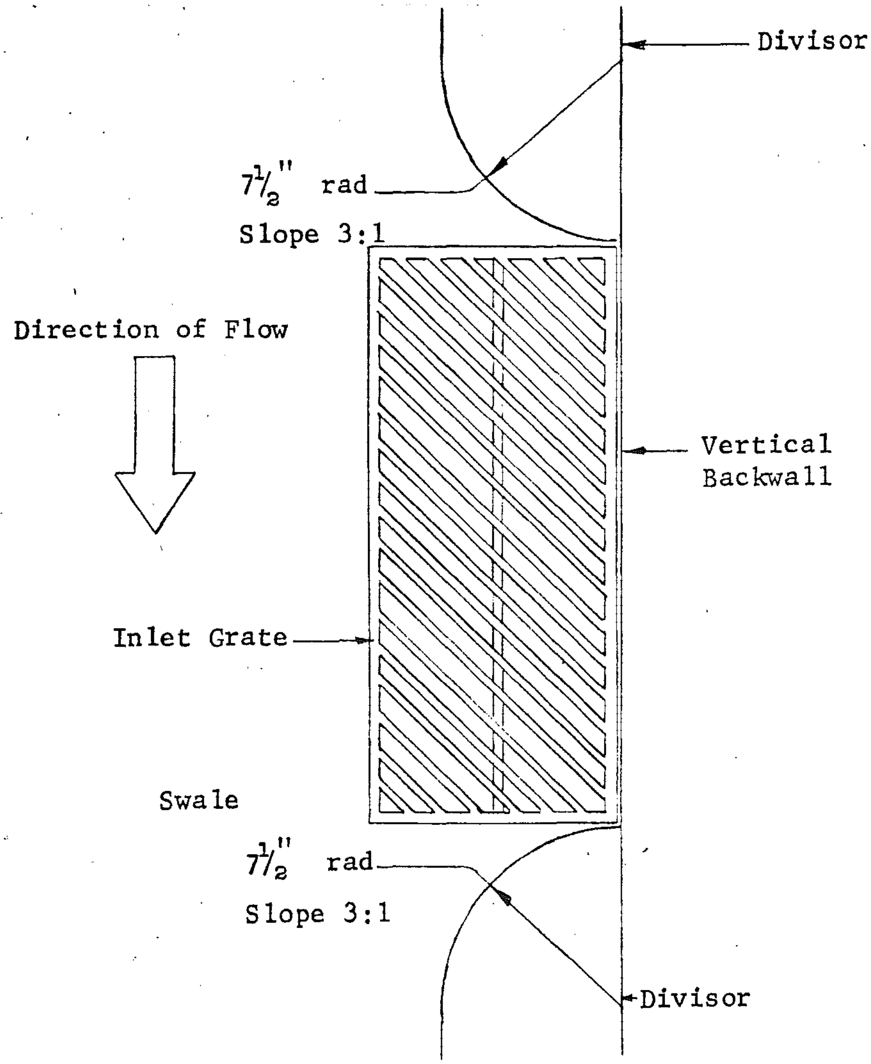

(a) Plan View

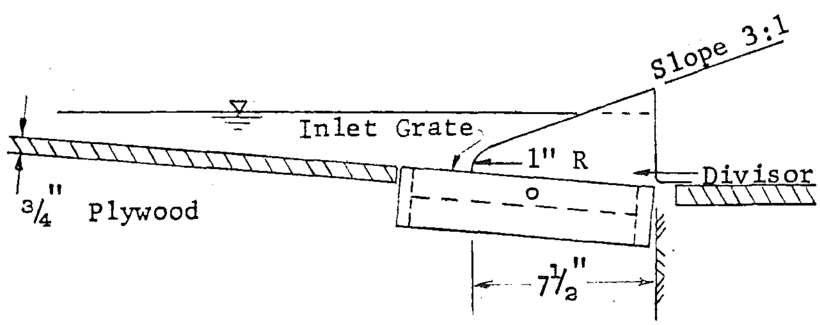

(b) Elevation View

Fig. 3.3 Installation for Type J Inlet

3.2 Laboratory Equipment

3.2.1 General Requirements

A full-size inlet grating was considered ideal in performing the experiments. However, as mentioned in Section 2.1, this could not be attained owing to the existing facilities and to the maximal discharge available in the laboratory. Hence, a prototype:model ratio of 2:1 was selected.

In order to obtain uniform flow in the channel upstream from an inlet, one would require a relatively long channel with a minimal amount of channel distortion. Guide vanes and baffles might be used in order to improve the upstream condition.

The frame supporting a model should be rigid. On the other hand, the model itself must be made versatile, because the experiments to be performed must involve different longitudinal slopes, swale slopes, and back slopes. The mechanism used to change these slopes should be simple and rugged. The model itself should be fabricated so that the change of inlet gratings would require a minimum of modification.

The surface roughness of the channel should bear a close resemblance to that of the pavement as used by the Pennsylvania Department of Transportation. The Manning coefficients for the model pavement and for the prototype pavement should be as similar as possible. The Manning coefficient of the material used in the model channel would have to be determined in a testing flume (see Section 2).

Inasmuch as the paramount objective of the study would be to determine the efficiencies of different inlets under a variety of conditions, efforts should be made to ensure that absolutely no leakage of water occur in the entire system and that measurements of flow rate be as accurate as possible.

3.2.2 Apparatus

A schematic diagram of the testing arrangement is shown in Fig. 3.4. Two pumps (B) raise water from the main sump (A) into the pressure tank (D). The two pumps can be operated either in parallel or in series by adjusting the three valves (C).

Each pump is driven by a Westinghouse 9B Type HF Induction Motor equipped with a rheostatic control. One motor had a rating of 40 Hp with a maximal speed of 1740 rpm; the other motor had a rating of 35 Hp with a maximal speed of 1720 rpm. The system operates on 220 volts AC. During a test both motors were adjusted to a rate of discharge that was fairly constant over a period of time.

Each pump is a single-stage, double-suction, centrifugal pump, Type I of DeLaval Manufacture. One pump had a 10-inch suction line and an 8-inch discharge line, whereas the other pump had an 8-inch suction line and a 6-inch discharge line.

The circular pressure tank (D) is $5\frac{1}{2}$ feet in diameter and 34 feet high. The rate of discharge delivered to the manifold discharge pipe (M) in the head tank (N) was obtained by opening the supply valve (E). The rate of inflow was measured by means of a

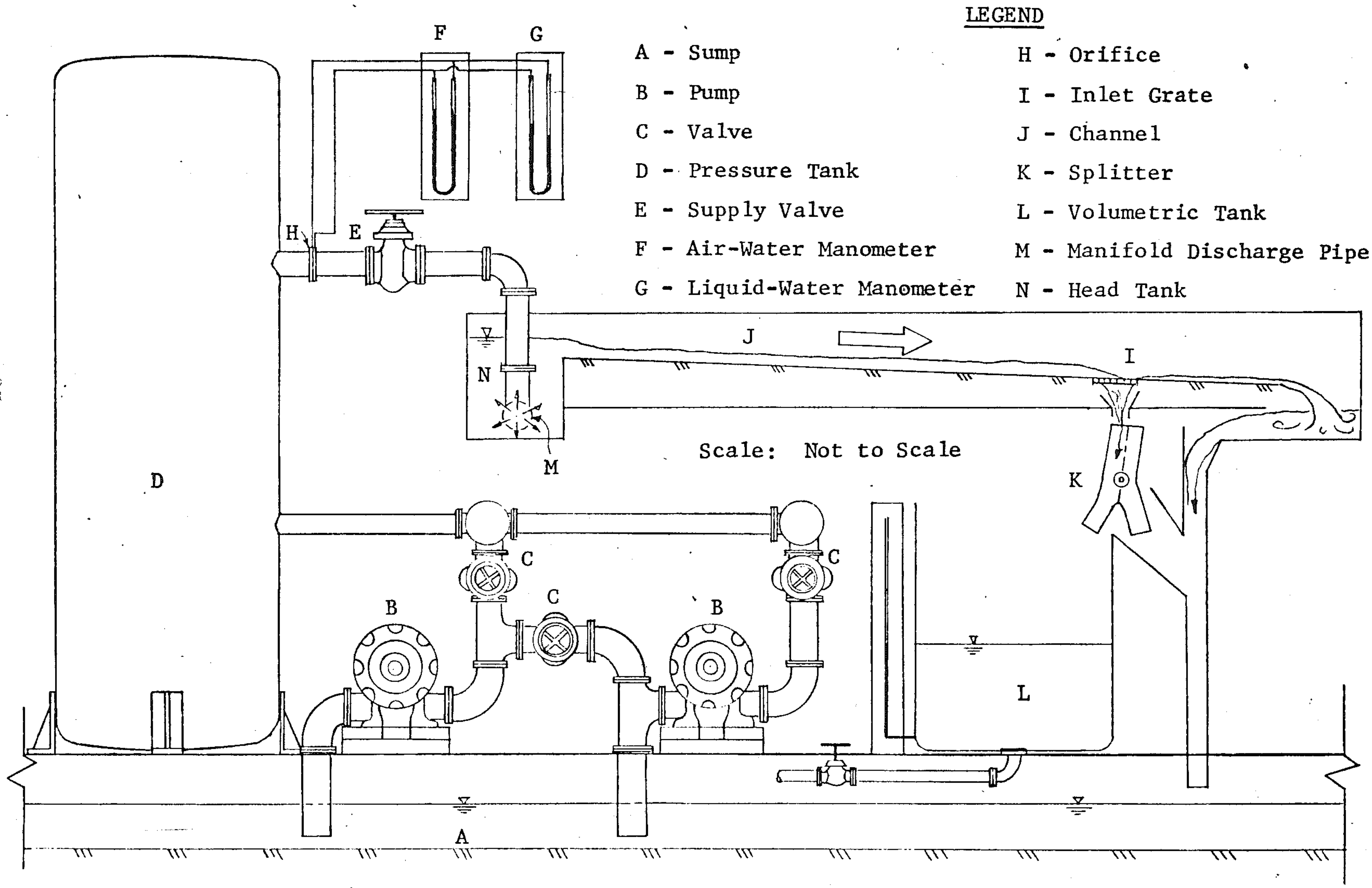

Fig. 3.4 Schematic Diagram

4-inch orifice (H) placed upstream from the supply valve in a 12-inch pipe, using either an air-water manometer (F) for a discharge of $Q \leq 0.5$ cfs or by a liquid-water manometer (G) for a discharge of $Q > 0.5$ cfs. The manometer liquid had a specific gravity of 2.95. The 4-inch orifice had been calibrated previously with the resulting volumetric expression given as:

$$Q = 0.42 \; H^{1/2}, \tag{26}$$

where Q is the flow rate of water in cubic feet per second, H is the pressure-head difference across the orifice in feet of water. Equation (26) was found to be correct when the orifice was recalibrated once again after some inlets had been tested.

As soon as the water was delivered into the head tank (N), it flowed through the channel (J) toward the inlet (I). The amount of water intercepted by the inlet was guided by the splitter (K) into the volumetric tank (L), if a measurement of rate of interception was taken, or was returned immediately into the main sump (A). The volumetric tank has a capacity of about 450 cubic feet. The amount of carryover flowed directly back into the sump (A).

The testing tank is rectangular in shape (see Fig. 3.5) and made of 1/4-inch steel plate framed by 3-inch by 3-inch angle iron. The bottom of the tank rests on beams placed transversely on 4-foot centers along the entire length of the testing tank. These beams are 2-inch by 7-inch channels. The testing tank has a total length of 33 feet, a width of 16 feet, and a depth of 3 feet. The head tank

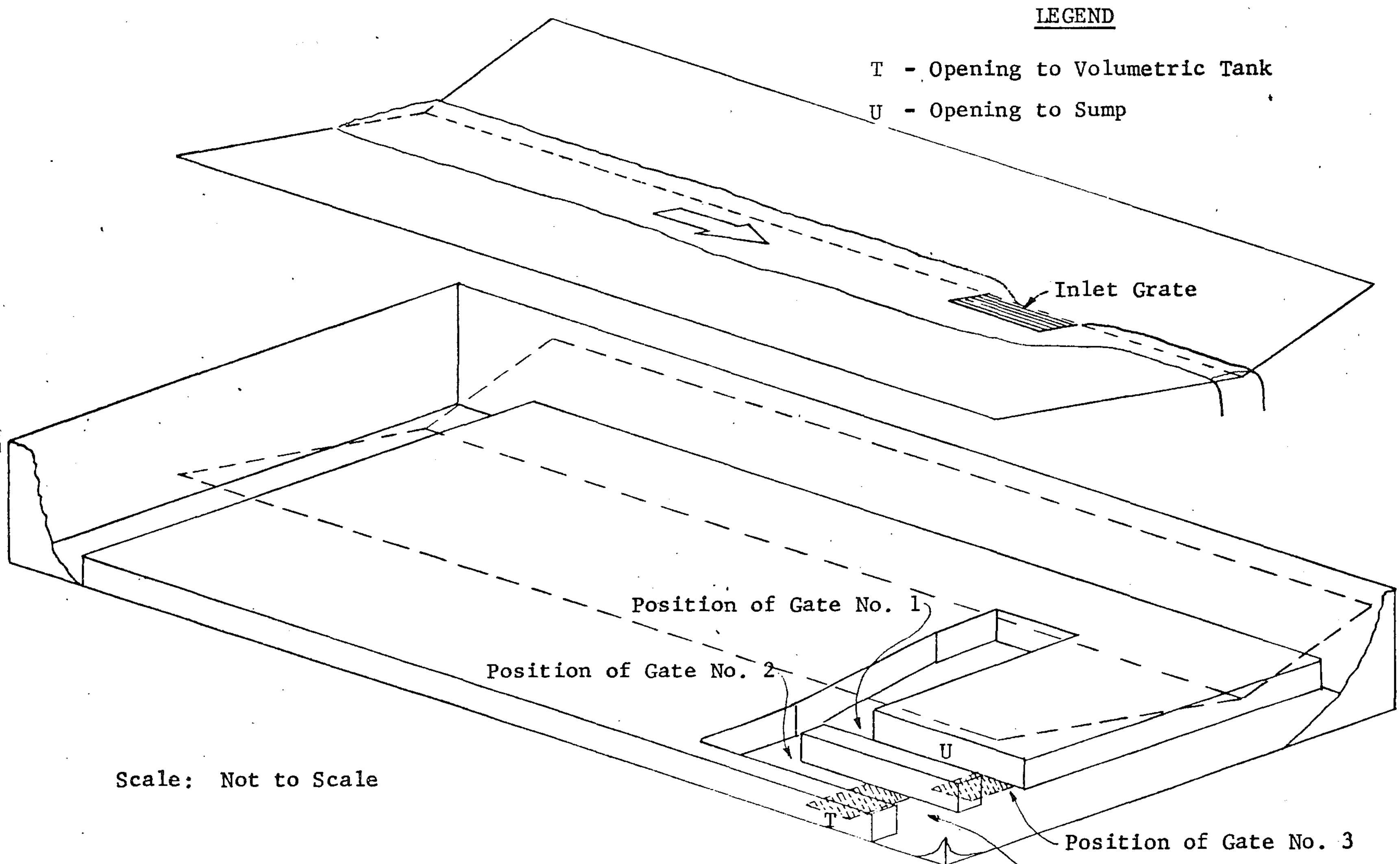

Fig. 3.5 Cutaway View of Testing Tank

containing the manifold discharge pipe is $2\frac{1}{2}$ feet long, 16 feet wide, and 4 feet deep.

Figure 3.5 is a cutaway view of the testing tank, and Fig. 3.6 shows the model placed in the testing tank. A conveyance channel (R), 1-foot deep with an average width of 2 feet, carries the water intercepted by the drainage inlet to an opening (T) connected to a volumetric tank. Another opening (U) near the downstream end of the testing tank is connected to the main sump.

During the process of calibrating the orifice, gates 1 and 3 were closed so that all water was drained into the volumetric tank through the opening (T) for measurement. To determine the amount of water intercepted by the inlet, gates 2 and 3 are opened while gates 1 and 4 are closed, whereas to determine the amount of carryover, gates 2 and 3 are closed and gates 1 and 4 are open.

3.2.3 Model Construction

Two steel frames were constructed to support the swale (O) and back slope (P) which form a triangular channel. One frame is 28 feet long and 12 feet wide, and the other is 28 feet by $3\frac{1}{2}$ feet. The former represents a portion of the swale of the roadway while the latter one represents a back slope. Both frames were made of S4 x 9.5 I-beams welded together. The welded joints were reinforced by clip angles in order to prevent any failure and to minimize deflection. The outer edges of the frames were made of S7 x 15.3 I-beams.

Both frames were covered with 3/4-inch outdoor plywood; each piece, measuring 4 by 8 feet, was treated with one coat of preservative and with two coats of enamel paint. The joints of the plywood were covered with a 2-inch self-sticking transparent tape. The tape was then later covered with an enamel paint. Hinges were welded to the invert of the channel in order to prevent the two steel frames from separating and to provide freedom for the frames to rotate about the invert whenever different side slopes were desired.

The entire length of the invert rests on a W8 x 40 I-beam (S). This main supporting I-beam (see Fig. 3.6) is 28 feet in length and is hinged at its downstream end. By providing the proper height of support at the upstream end of the I-beam, any amount of longitudinal slope of the channel could be obtained to a maximal slope of 8.0%. Mid-point deflection of the I-beam was virtually eliminated by providing support at mid-span. The outer edge of the two frames is supported by four 3/4-inch threaded tension rods (Q). Hence, each side slope can be raised or lowered independently of the other. For structural reasons part of the main supporting I-beam is below the inlet gratings. Although this is not desirable because the beam could affect the flow pattern of the water coming into the inlet, efforts were made to ensure the vertical distance between the inlet opening and the beam be the maximal possible. Observation during testing showed that the I-beam was insignificant in affecting the flow.

Baffles and 30 aluminum guide vanes were installed at the upstream end of the channel so as to aid in developing uniform flow as the water approached the inlet. The guide vanes, each measuring 2 feet by 6 inches, were placed on 2-inch centers.

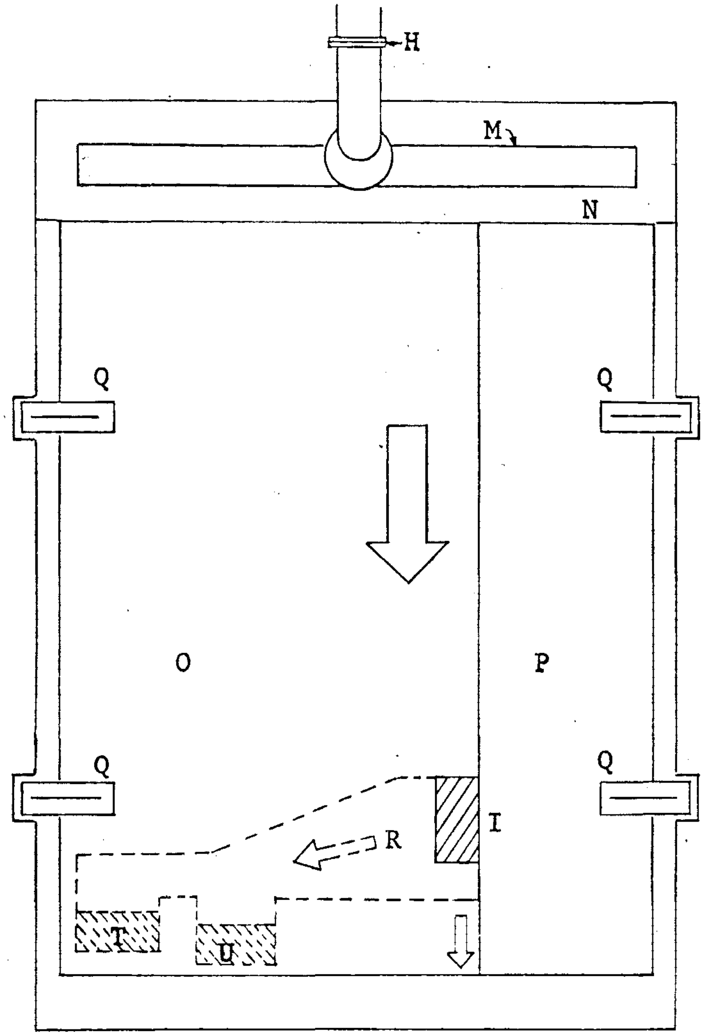

(a) Plan View

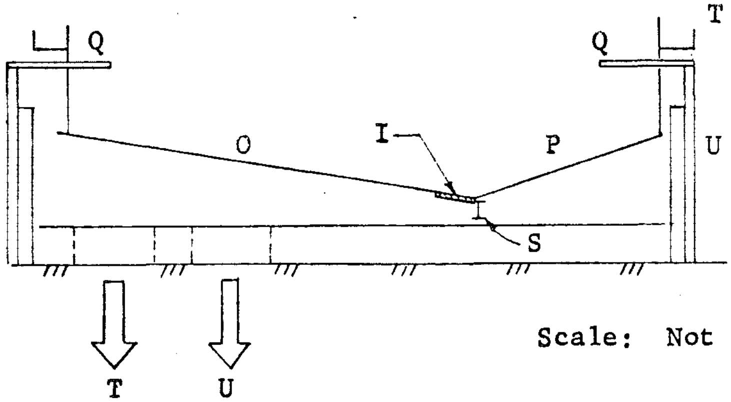

(b) Elevation View

LEGEND

H - Orifice

M - Manifold Discharge Pipe

N - Head Tank

O - Swale Slope

P - Back Slope

Q - Side-Slope Adjustment Rods

R - Conveyance Channel

S - Main Supporting I-Beam

I - Inlet Grates

T - Opening to Volumetric Tank

U - Opening to Sump

Scale: Not to Scale

Fig. 3.6 Testing Tank with Channel and Inlet Grate

3.3 Technique

3.3.1 Flow Measurements

As mentioned in Section 3.2.2, the flow rate into the head tank (N) was determined by reading the pressure-head difference across the 4-inch orifice indicated in the differential manometers (F) and (G). The orifice had previously been calibrated by a standard volumetric measuring method. The air-water manometer was used exclusively at discharge rates lower than 0.5 cfs because it yielded much more accurate results when the pressure drop across the orifice was small. The maximal discharge for the 4-inch orifice was 1.65 cfs. A higher discharge could be obtained by either (a) using a larger orifice, or (b) increasing the supply valve opening, or (c) increasing the speed of the motors.

The water intercepted by the drainage inlet is directed into the volumetric tank after properly positioning the four gates in the conveyance channel. This amount of water intercepted by the inlet can be obtained by recording the difference of the water level in the volumetric tank. The flow rate (Q_2) is the amount of water intercepted divided by the time interval involved. The carryover flow rate (Q_3) is the difference between the channel or supply flow rate (Q_1) and the intercepted flow rate (Q_2). The water in the volumetric tank is drained periodically into the main sump by opening the drainage valve.

3.3.2 Depth Measurements

A point gage graduated to 0.001 ft was used in all depth measurements. The gage is mounted on a small carriage that rolls along a 3-inch by 5-inch aluminum rectangular channel which is 17 feet long, is placed 2 feet above the invert, and is at right angles to the invert of the channel. Both ends of the aluminum member are supported by a monorail system which permits the beam to travel freely above the invert of the channel. Such an arrangement permits a depth measurement to be made at any point in the channel. During a test measurements of depth were taken at stations that were 1 ft, 2 ft, and 3 ft upstream from the start of inlet gratings.

3.4 Steady, Uniform Flow

Steady, uniform flow is a requirement for an investigation such as this one. Such a flow condition is not present at the entrance to drainage inlet owing to the water converging toward the opening in the lateral as well as in the vertical directions.

One indication of the desired flow is a cross-sectional area of flow having a constant shape. In a triangular channel this is clearly shown by the spread of the water surface on the flatter or swale slope. Accordingly the spread of the water surface from the invert was measured at the cross section where the depths were measured; that is, the lateral extent of the water was measured at distances of 1 ft, 2 ft, and 3 ft, upstream from the start of the inlet. The numbers obtained are listed on the sheets of the experimental data.

3.5 Procedure

Prior to a test, the particular inlet grating was installed according to PennDOT specifications. The channel configurations (longitudinal slope, swale slope, and back slope) were then adjusted and checked with the use of a surveyor's level.

Subsequently the supply valve (see Figure 3.4) was opened to a certain flow rate (Q_1) which was obtained by reading the pressure drop across the orifice from the manometers; equation (26) was used to calculate Q_1.

A suitable time-interval (5 minutes was found to be usually sufficient) elapsed until steady-state condition was obtained in the channel. Subsequently the depth measurements were made. The amount of water intercepted by the inlet during one minute was guided by the splitter into the volumetric tank for determination of the intercepted flow rate, Q_2. By subtracting the intercepted flow rate (Q_2) from the supply flow rate (Q_1), the carryover flow rate (Q_3) was obtained.

After all measurements corresponding to one flow rate were recorded, the incoming flow was slightly decreased by closing the supply valve, and the entire procedure was repeated. Usually 10 different flow rates sufficed to define the inlet efficiency curve. The experimental data are summarized in the Appendix.

4. RESULTS AND DISCUSSION

4.1 Experimental Results

All measurements made in this study are presented in the Appendix. They are also displayed in Figures 4.1 to 4.12 and summarized in Tables 4.1 to 4.3.

The schedule for the tests was arranged in such a way that a minimum of alteration and the least amount of time were required in order either to change inlet gratings or to alter the three slopes of the channel. A few tests were repeated owing either to inadequate data points or to unsatisfactory results.

The efficiency of an inlet, indicated as η, is defined as $(Q_2/Q_1) \times 100\%$, where Q_1 is the channel flow rate (discharge) in cfs, and Q_2 is the intercepted flow rate in cfs. The efficiency curves for the inlets are presented in Figures 4.1 to 4.12, inclusive. The channel flow rate, Q_1, is plotted on the lower horizontal axis against the efficiency in percent on the vertical axis. The upper horizontal axis represents the prototype channel flow rate, Q_1; this quantity in relation to the model channel flow rate is obtained by using Eq. (20a).

Each figure shows the efficiencies of an inlet for one particular channel longitudinal slope and one back slope, but with four different swale slopes, namely, 12:1, 16:1, 24:1 and 48:1. The three dashes on a curve show that a water spread of 8 feet is reached on the swale in the prototype channel, or a spread of 4 feet on the swale in the model channel. The absence of the three dashes on a curve indicates that the spread of 4 feet on the swale of the model channel was not obtainable.

4.2 Discussion of Measurements

4.2.1 Flow Measurements

The use of an orifice placed in a pipe to measure channel flow rate yielded accurate results. The range of channel flow rates was from 0.038 cfs to 1.65 cfs. Eq. (26) was used to calculate the channel flow rate after obtaining the pressure drop across the orifice. The equation was corroborated by recalibrating of the orifice, provided the motor of each pump was set to the same speed every time as that during orifice calibration.

In order to obtain an efficiency of 100 percent for an inlet placed under a certain condition, it was necessary to reduce the flow so that no water would by-pass the inlet. Such condition was usually obtained by actual observation at the downstream side of the channel. Since one drainage inlet (Type J) has fairly low efficiencies, particularly at a steep channel slope and a flat swale slope, it was at times difficult to adjust the flow so that 100 percent efficiency was obtained.

The intercepted flow rate was obtained by means of a volumetric measurement over a period of time, usually 60 seconds. It was found that such a time interval was adequate.

4.2.2 Depth Measurements

As mentioned in Section 3.2.2, all depth measurements were obtained by means of a point gage. Depths were measured at the invert of the channel. Three depth readings for each channel flow rate were taken at stations that were 1 ft, 2 ft, and 3 ft horizontally upstream from the upper end of the inlet grating; the readings were recorded on data sheets in that order. If the slope of the channel was steep and the channel flow rate high, it was difficult to take any depth measurement accurately due to the fluctuation of the water surface about some mean point.

Guide vanes were used at the upstream end of the channel so as to aid in developing uniform flow (see Section 3.2.3). However, they could not completely eliminate some surface cross waves which might have affected the depth readings. It was found that baffles placed at the upstream portion of the channel were quite satisfactory in eliminating surface cross waves. The baffles were made of ¼-inch galvanized hardware cloth that was deformed and then placed in layers so as to present in end view the configuration of 1-inch chicken wire, the layers being successively soldered together. At low flow rates over flat slope of the channel, such baffles were not essential.

4.3 Efficiencies of Inlets

The main purpose of this study is to determine experimentally the efficiencies of three highway drainage inlets used by the Pennsylvania Department of Transportation under various channel configurations and over a range of channel flow rates. Inasmuch as most standard inlets are constructed and installed differently, they will have different efficiencies when tested under the same condition. Obviously an inlet having a larger opening will intercept more water than one having a smaller opening. Hence it is only reasonable to compare the performances of any particular inlet under certain different channel configurations.

By observation of the efficiency curves shown in Figures 4.1 through 4.12, a general conclusion can be made: for an inlet placed in a channel with fixed longitudinal and back slopes, its efficiency decreases as the steepness of the swale slope decreases for the same channel flow rate. The reason is that the spread of water on the swale slope is much smaller for a steep swale slope than for a flat swale slope. Consequently a transition, where possible, from a flat swale slope to a steeper one upon approaching an inlet would improve its efficiency.

4.3.1 Efficiencies of Type J Inlet

Figures 4.1 through 4.4 show the efficiency curves for Type J Inlet. It can be noted that without a change in the channel configuration, the efficiency of an inlet drops as the channel flow rate increases. At low channel flow rates where the efficiencies are high, all curves drop drastically as the channel flow rates are increased; this is an area of steep curves. Upon increasing the channel flow rates, the steepness of these efficiency curves are reduced and they tend to be parallel to one another at high channel flow rates; this is an area of less steep curves.

The longitudinal slope of the channel also has a significant effect on the efficiency of the drainage inlet. If the longitudinal slope of the channel is steep, some water, owing to its high inertia, flows along the top surface of the grating; thus it by-passes the inlet. This indicates a need to cause the water to be deflected into the inlet. The highest efficiency for the Type J Inlet generally occurs where the inlet is installed on a longitudinal slope of $\frac{1}{2}\%$.

The efficiency of Type J Inlets depends also upon the channel flow rate. Observations pertaining thereto are summarized in Table 4.1, wherein columns 1 and 2 describe the configurations of the channel. Columns 3 and 4 indicate, respectively, the capacity of an inlet for an efficiency of 100% and the efficiency of an inlet for a flow rate 50% greater than that of column 3. In general the efficiencies of the Type J Inlets are very low. For a grade of 8 % and steep swales, increasing the flow from that at 100% efficiency to 1.5 that amount leads to a reduction in efficiency of 50%. Although that drop in efficiency is not so marked for the other grades, all of this does signify that increasing the width of the inlet could lead to an increase in efficiency.

4.3.2 Efficiencies of 4-Ft Special Inlet and 6-Ft Special Inlet

Figures 4.5 through 4.8 show the efficiency curves of the 4-Ft Special Inlet. whereas Figures 4.9 through 4.12 show the efficiency curves of the 6-Ft Special Inlet. Type 6-Ft Special Inlets have usually higher efficiencies than the 4-Ft Special Inlets provided both are placed under the same channel condition and flow rate. However the difference in efficiencies between the two inlets is so small as to lend substance to the conclusion that the inlets can be used interchangeably.

All figures show almost an absence of area of steep curves as discussed in Section 4.3.1. However, it can be noticed that for the same channel condition curves corresponding to different swale slopes are parallel to one another, or tend to be so. Figures 4.5 through 4.8 show that for the Type 4-Ft Special Inlet in a channel with fixed longitudinal slope and back slope the efficiency increases:

1. Between 12% and 20% for a change of swale slope from 48:1 to 24:1;
2. Between 5% and 18% for a change of swale slope from 24:1 to 16:1; and
3. Between 2% and 10% for a change of swale slope from 16:1 to 12:1.

Figures 4.9 through 4.12 show that for the Type 6-Ft Special Inlet in a channel with fixed longitudinal slope and back slope, the efficiency increases:

1. Between 12% and 20% for a change of swale slope from 48:1 to 24:1;
2. Between 4% and 18% for a change of swale slope from 24:1 to 16:1; and
3. Between 4% and 10% for a change of swale slope from 16:1 to 12:1.

In general, channels having a longitudinal slope of either 2% or 4% yield much higher inlet efficiencies for both the 4-Ft Special Inlet and the 6-Ft Special Inlet than channels having a longitudinal slope of ½% or 8%.

Table 4.2 and Table 4.3 show the characteristics of the efficiency curves for the Type 4-Ft Special Inlet and for the Type 6-Ft Special Inlet, respectively. The Type 6-Ft Special Inlet always has a slightly higher capacity than the other inlet at an efficiency of 100% as shown in column 3 of each table. Further the efficiency of each inlet remains fairly high, above 90%, with an increase in the channel flow rate from $Q_{2_{100\%}}$ to $1.5Q_{2_{100\%}}$ as listed in column 4 of each table. These facts tend to indicate that the Type 4-Ft Special and the Type 6-Ft Special Inlets are satisfactory highway drainage inlets; the difference in efficiencies and capacities, being rather small, could permit the elimination of one of these two inlets from the Standard Drawings of PennDOT.

Long. Slope	Swale Slope	Q_2 @ η = 100% *	$1.5Q_2$
½%	12:1	0.679 cfs	η = 88%
"	16:1	0.566 cfs	η = 87%
"	24:1	0.475 cfs	η = 84%
"	48:1	0.215 cfs	η = 93%
2%	12:1	0.566 cfs	η = 80%
"	16:1	0.424 cfs	η = 77%
"	24:1	0.300 cfs	η = 85%
"	48:1	0.300 cfs	η = 70%
4%	12:1	0.475 cfs	η = 82%
"	16:1	0.368 cfs	η = 83%
"	24:1	0.368 cfs	η = 77%
"	48:1	0.300 cfs	η = 57%
8%	12:1	1.34 cfs	η = 50%
"	16:1	1.08 cfs	η = 50%
"	24:1	0.566 cfs	η = 51%
"	48:1	0.215 cfs	η = 59%

*η - Efficiency of inlet.
Q_2- Capacity of prototype inlet for an inlet efficiency of 100%.

Table 4.1 Comparison of Efficiencies of Inlet--Type J Inlet

Long. Slope	Swale Slope	Q_2 @ η = 100%*	$1.5Q_2$
½%	12:1	1.47 cfs	η = 98%
"	16:1	1.47 cfs	η = 94%
"	24:1	0.300 cfs	η = 98%
"	48:1	0.170 cfs	η = 97%
2%	12:1	2.77 cfs	η = 95%
"	16:1	2.07 cfs	η = 95%
"	24:1	1.78 cfs	η = 91%
"	48:1	0.600 cfs	η = 94%
4%	12:1	3.40 cfs	η = 89%
"	16:1	2.55 cfs	η = 92%
"	24:1	1.19 cfs	η = 93%
"	48:1	0.424 cfs	η = 96%
8%	12:1	2.41 cfs	η = 92%
"	16:1	1.95 cfs	η = 94%
"	24:1	1.22 cfs	η = 96%
"	48:1	0.453 cfs	η = 99%

*η - Efficiency of inlet.
Q_2 - Capacity of prototype inlet for an inlet efficiency of 100%.

Table 4.2 Comparison of Efficiencies of Inlet--4-Ft Special

Long. Slope	Swale Slope	Q_2 @ = 100% *	$1.5Q_2$
½%	12:1	2.66 cfs	η = 94%
"	16:1	1.47 cfs	η = 98%
"	24:1	0.940 cfs	η = 91%
"	48:1	0.215 cfs	η = 98%
2%	12:1	4.02 cfs	η = 93%
"	16:1	3.68 cfs	η = 86%
"	24:1	2.35 cfs	η = 87%
"	48:1	0.679 cfs	η = 95%
4%	12:1	4.08 cfs	η = 91%
"	16:1	2.89 cfs	η = 93%
"	24:1	1.55 cfs	η = 93%
"	48:1	0.662 cfs	η = 93%
8%	12:1	2.74 cfs	η = 94%
"	16:1	1.75 cfs	η = 96%
"	24:1	1.19 cfs	η = 97%
"	48:1	0.736 cfs	η = 97%

*η - Efficiency of inlet.
Q_2 - Capacity of prototype inlet for an inlet efficiency of 100%.

Table 4.3 Comparison of Efficiencies of Inlet--6-Ft Special

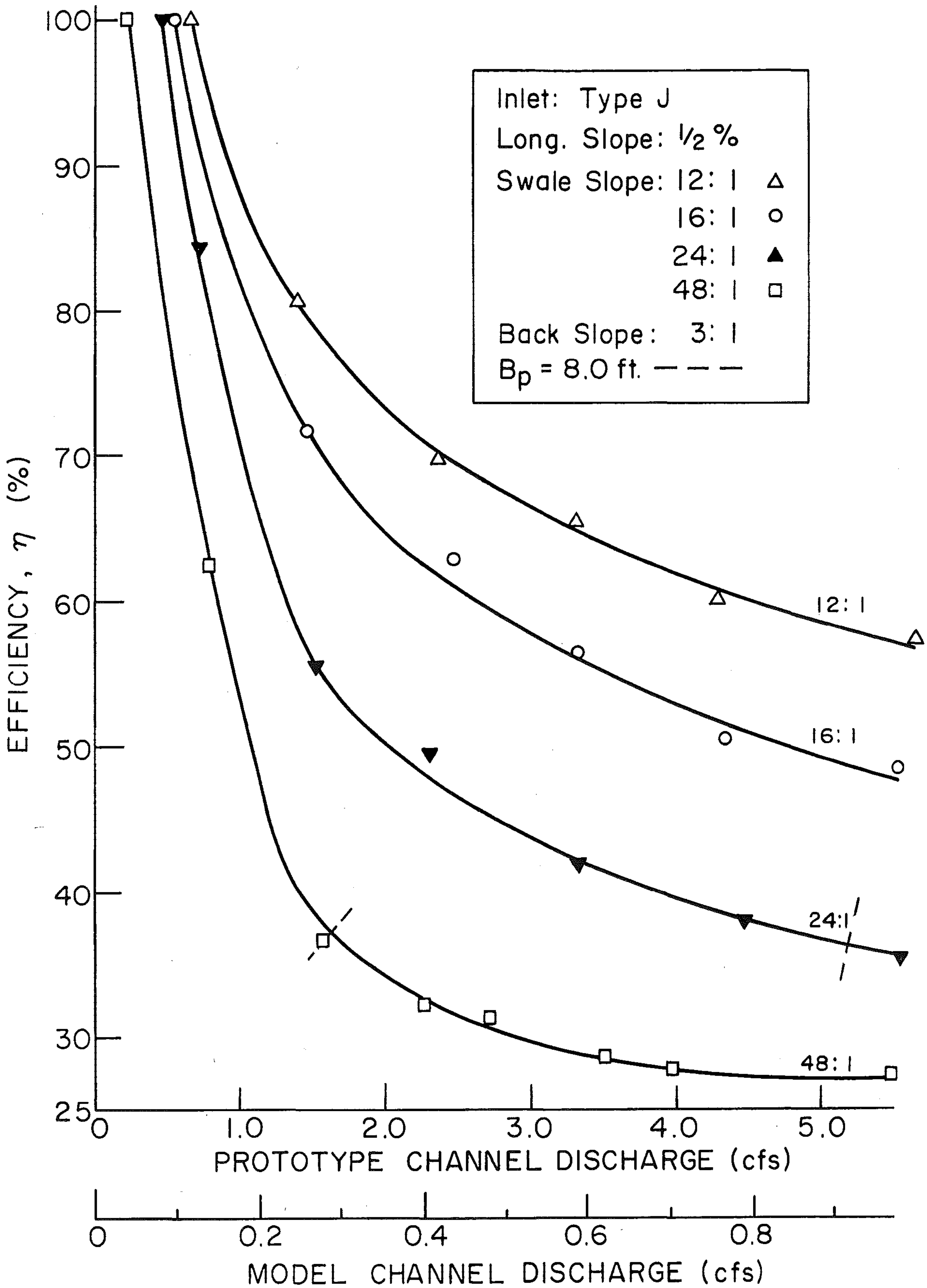

Fig. 4.1 Efficiency Curves; Type J Inlet (Long. Slope = ½%)

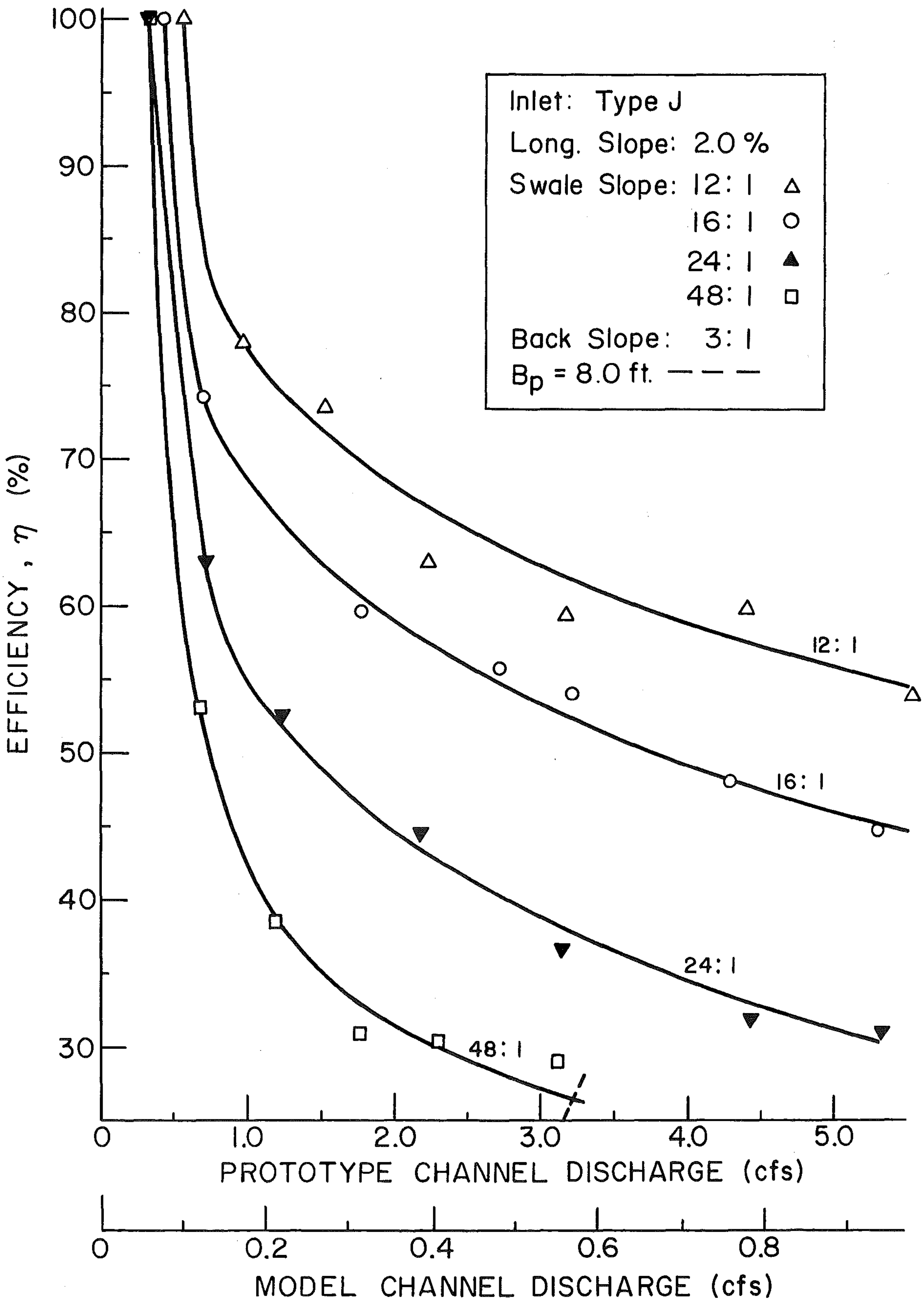

Fig. 4.2 Efficiency Curves; Type J Inlet (Long. Slope = 2%)

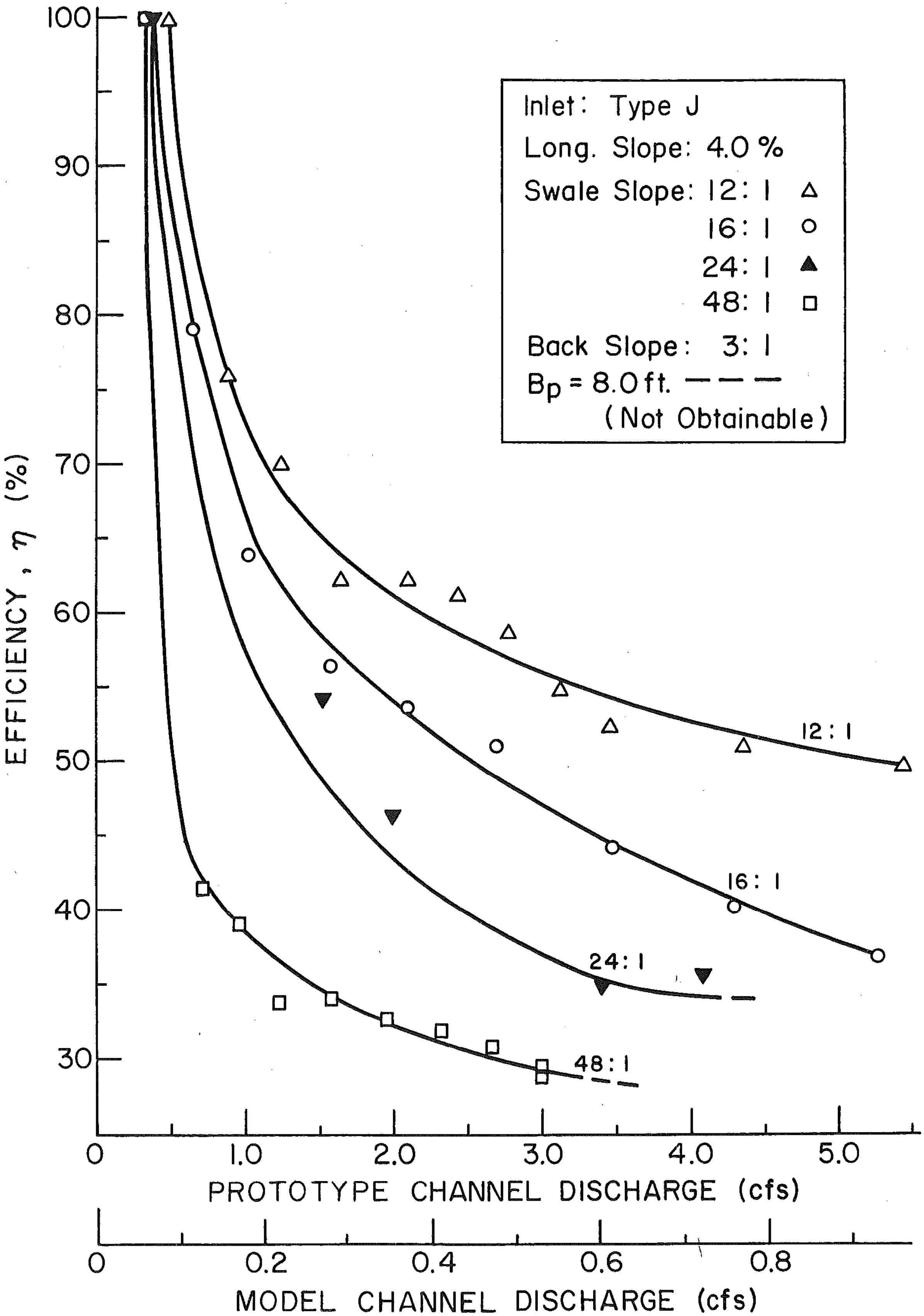

Fig. 4.3 Efficiency Curves; Type J Inlet (Long. Slope = 4%)

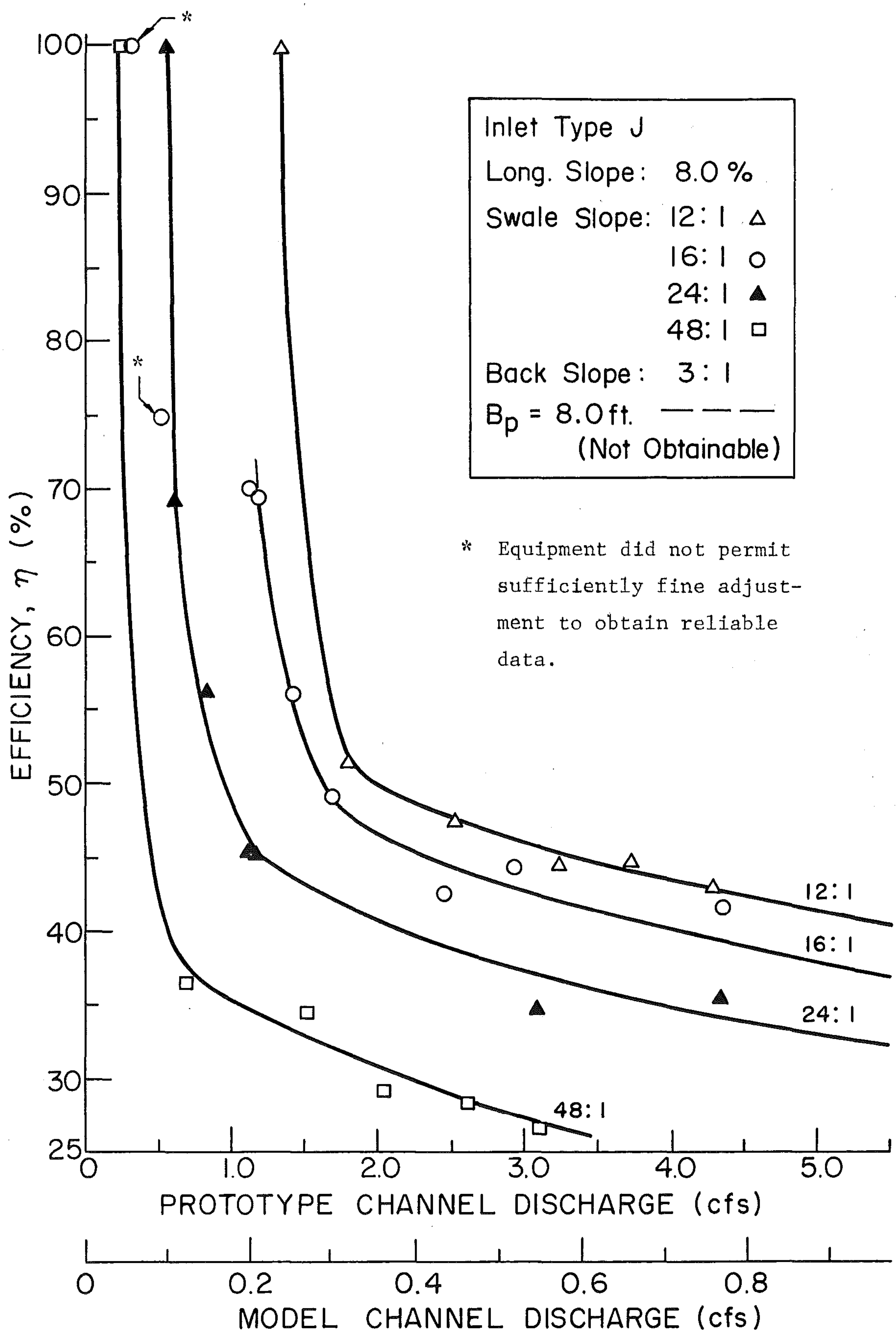

Fig. 4.4 Efficiency Curves; Type J Inlet (Long. Slope = 8%)

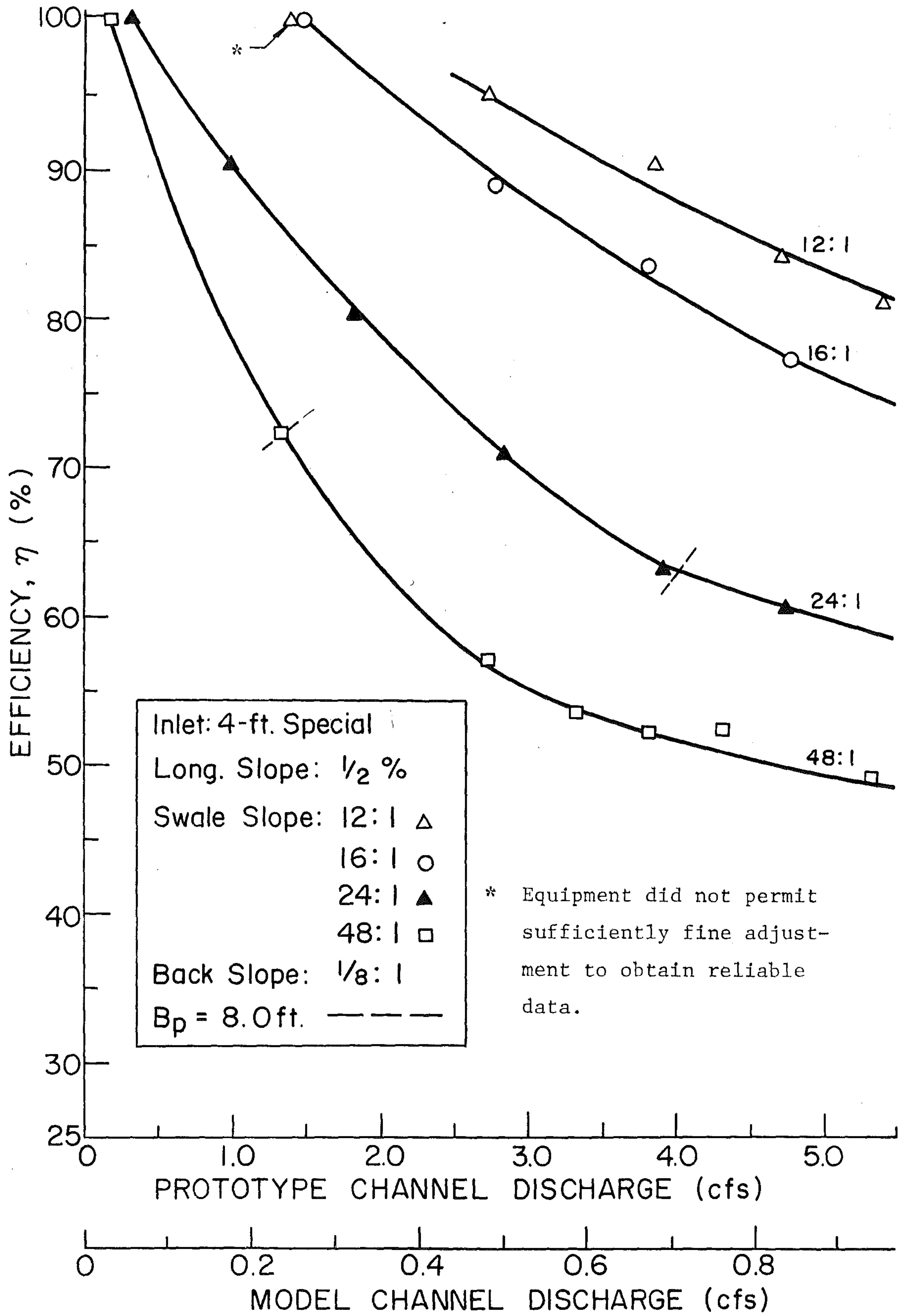

Fig. 4.5 Efficiency Curves; 4-Ft Special (Long. Slope = ½%)

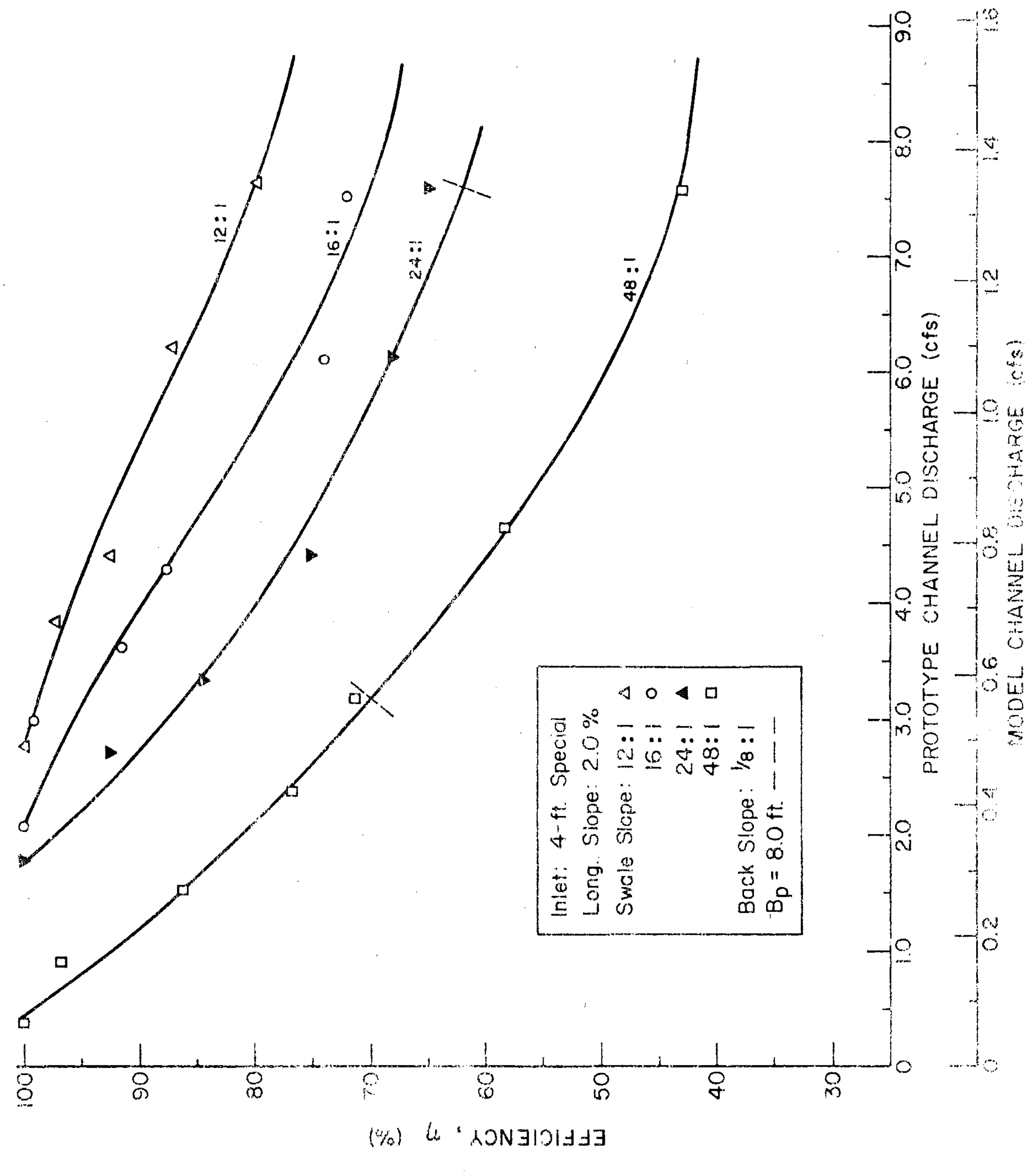

Fig. 4.6 Efficiency Curves; 4-Ft Special (Long. Slope = 2%)

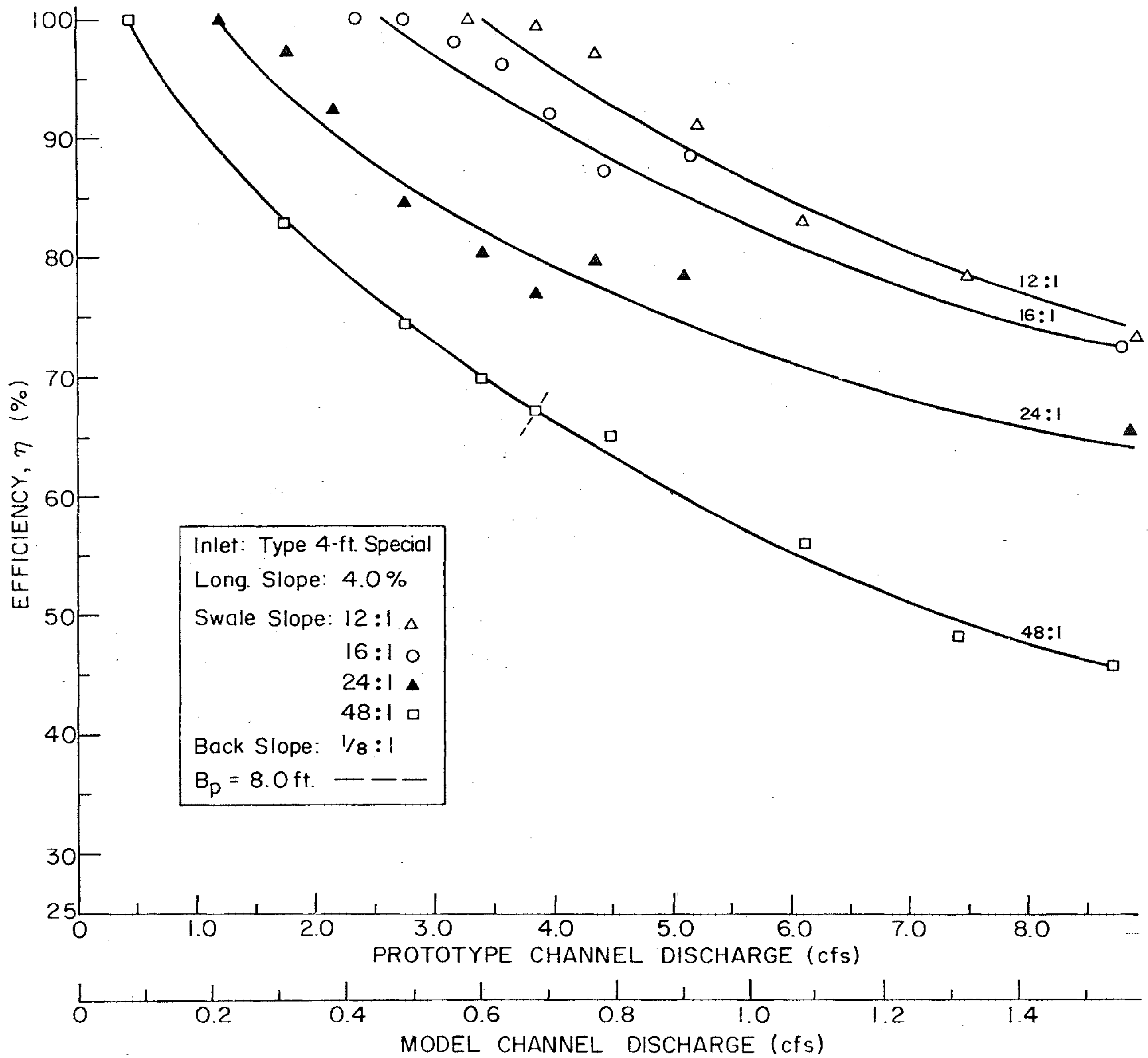

Fig. 4.7 Efficiency Curves; 4-Ft Special (Long. Slope = 4%)

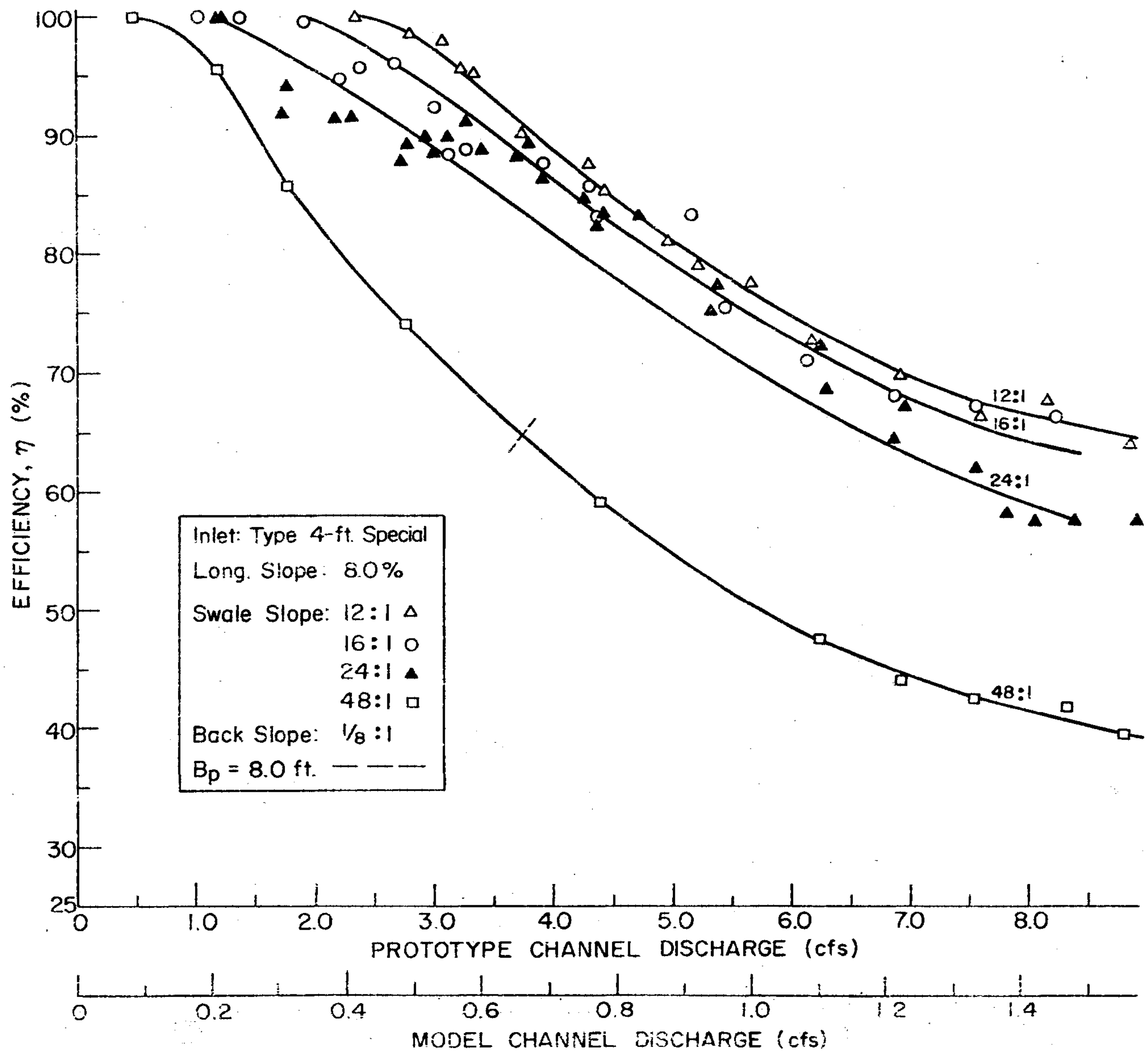

Fig. 4.8 Efficiency Curves; 4-Ft Special (Long. Slope = 8%)

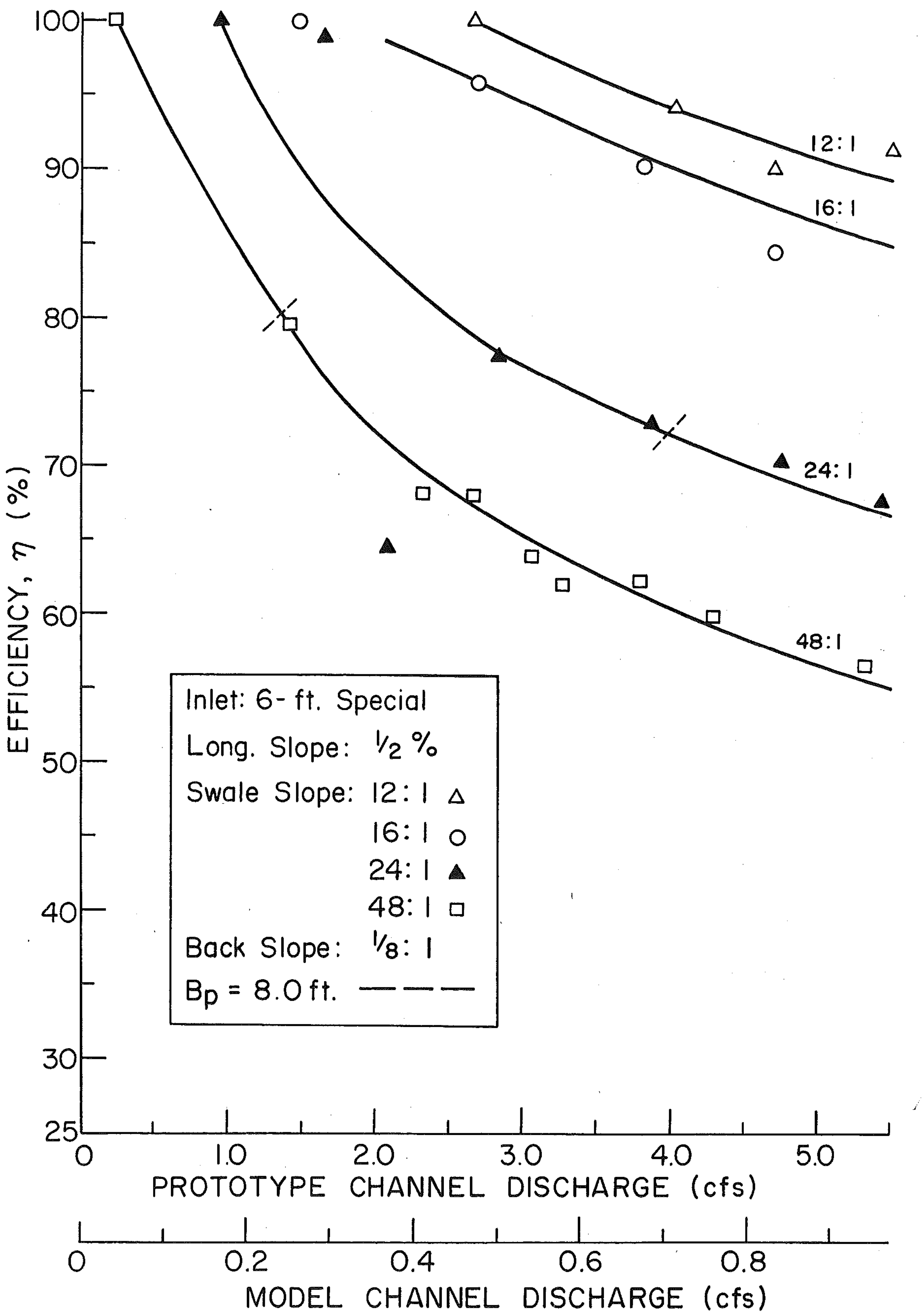

Fig. 4.9 Efficiency Curves; 6-Ft Special (Long. Slope = ½%)

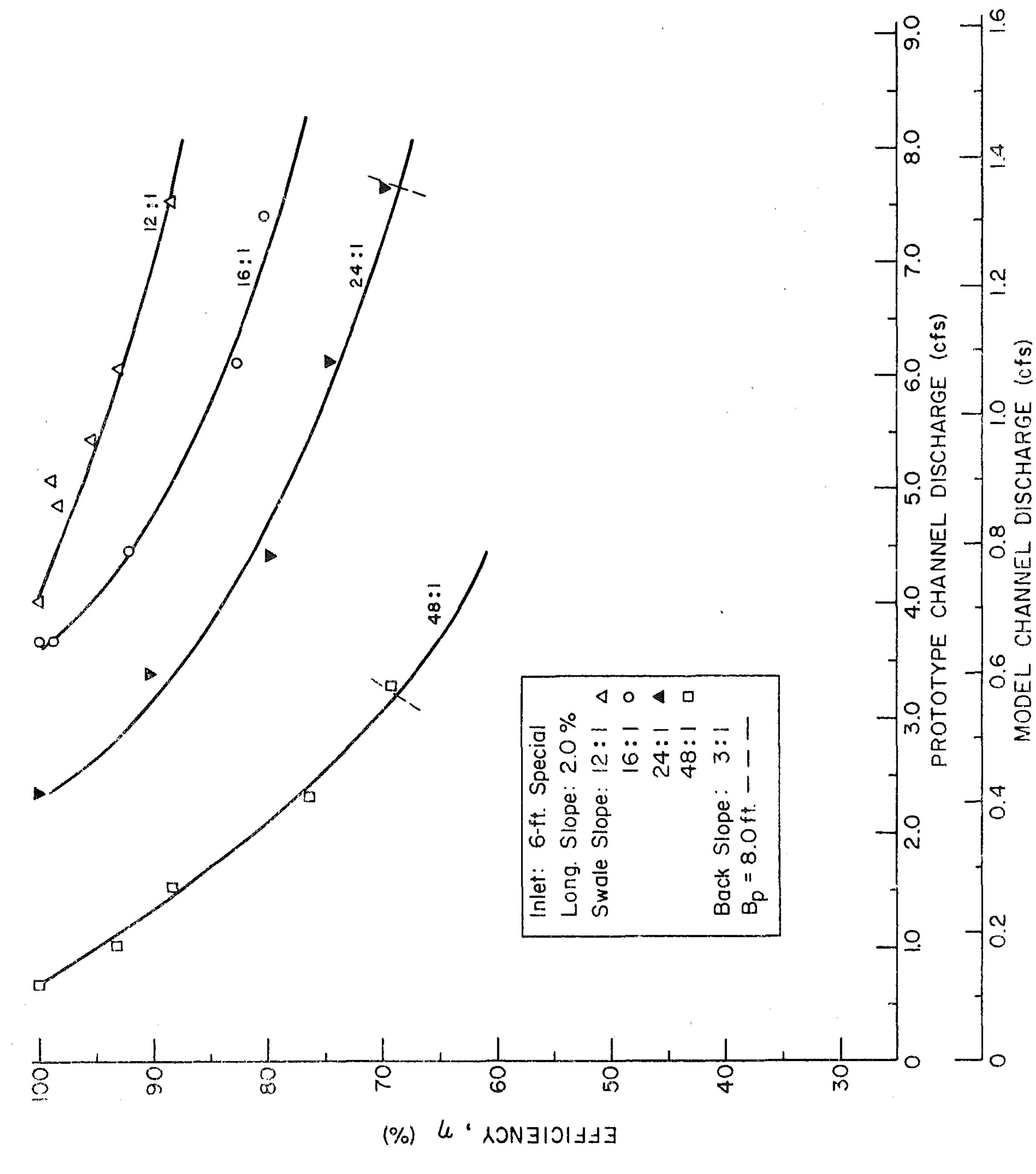

Fig. 4.10 Efficiency Curves; 6-Ft Special (Long. Slope = 2%)

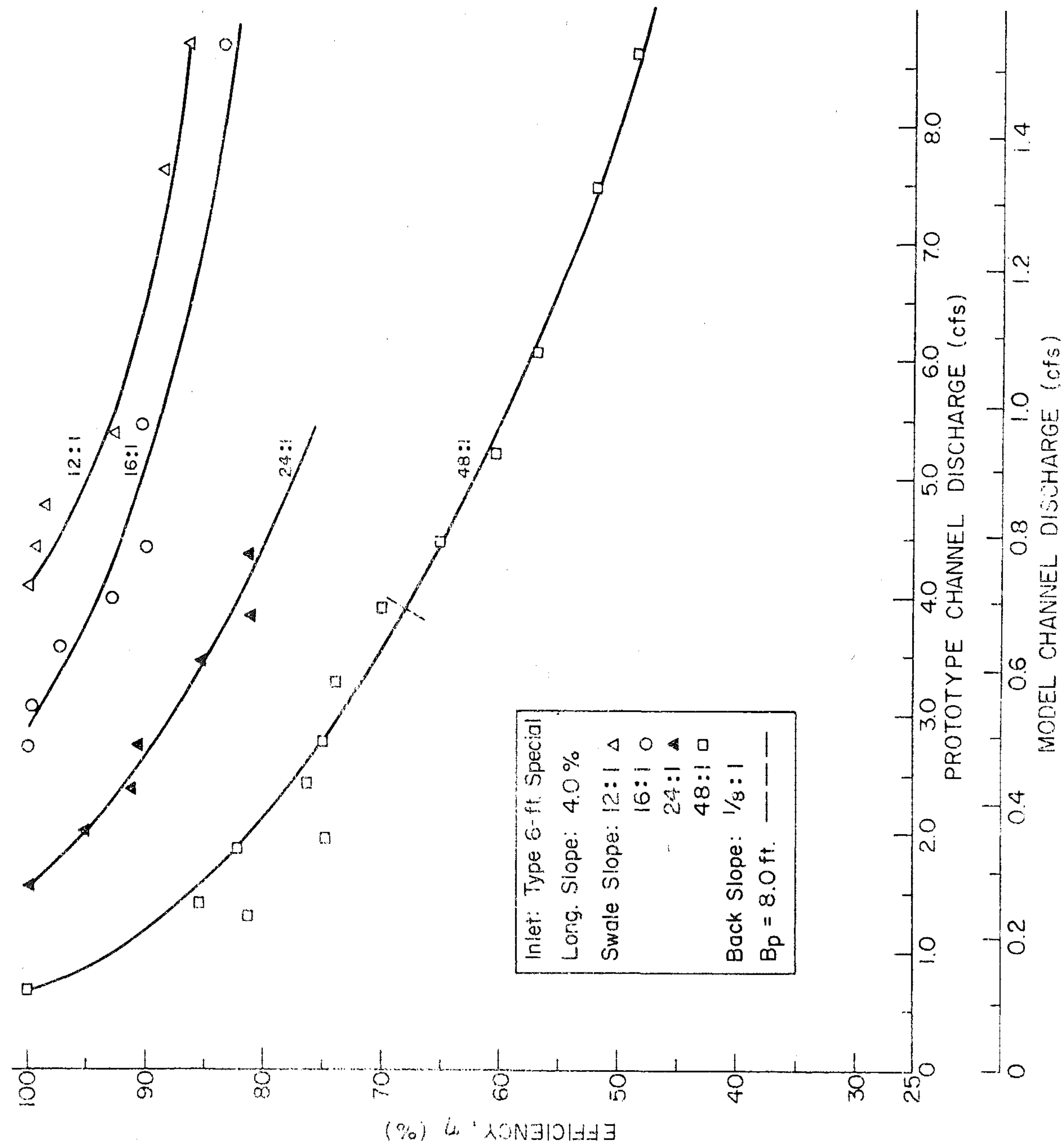

Fig. 4.11 Efficiency Curves; 6-Ft Special (Long. Slope = 4%)

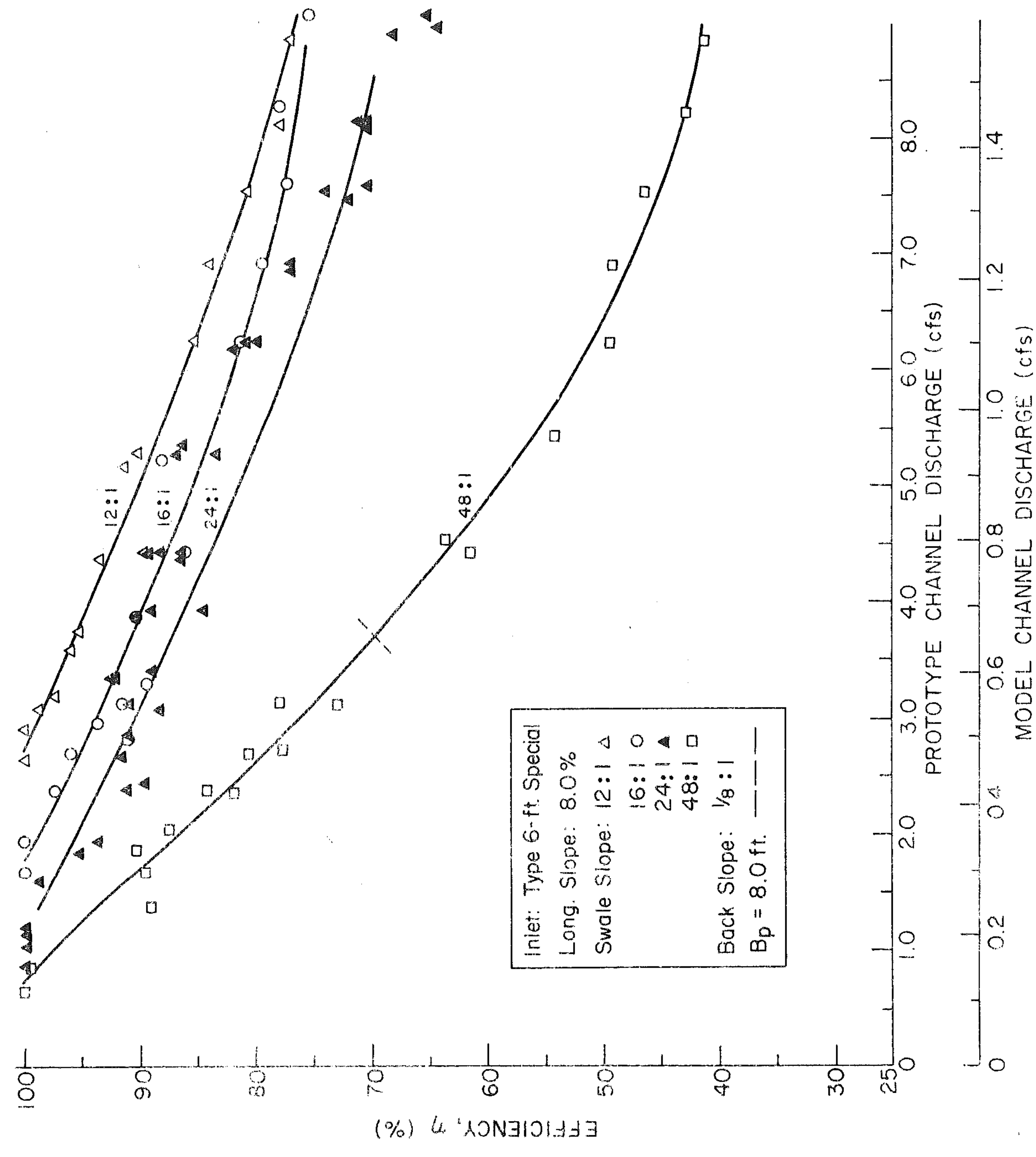

Fig. 4.12 Efficiency Curves; 6-Ft Special (Long. Slope = 8%)

5. SUMP EFFECT

5.1 General Remarks

A drainage inlet is usually installed at the lowest point of a vertical curve along a road. Such inlets have to drain away the water that flows toward the inlets from opposite directions along the channel; thus a sump effect occurs.

The sump effect was produced in the present experiments by installing a vertical barrier at the center of the inlet, the barrier being at right angles to the channel. Water was then introduced from the upstream end of the channel, and only the upstream one half of the inlet opening was effective in draining the water while the other half was inoperative.

The longitudinal slope of the channel was set at 0.2% and a vertical barrier, 8 inches in height and 12 feet in width, was installed as shown in Fig. 5.1. The data obtained from the tests are plotted in the form of curves, see Fig. 5.2 , 5.3 , and 5.4 , which relate the depth of the water along the invert of the channel one foot upstream from the drainage inlet to the volumetric rate of flow for swale slopes of 12:1, 16:1, 24:1, and 48:1.

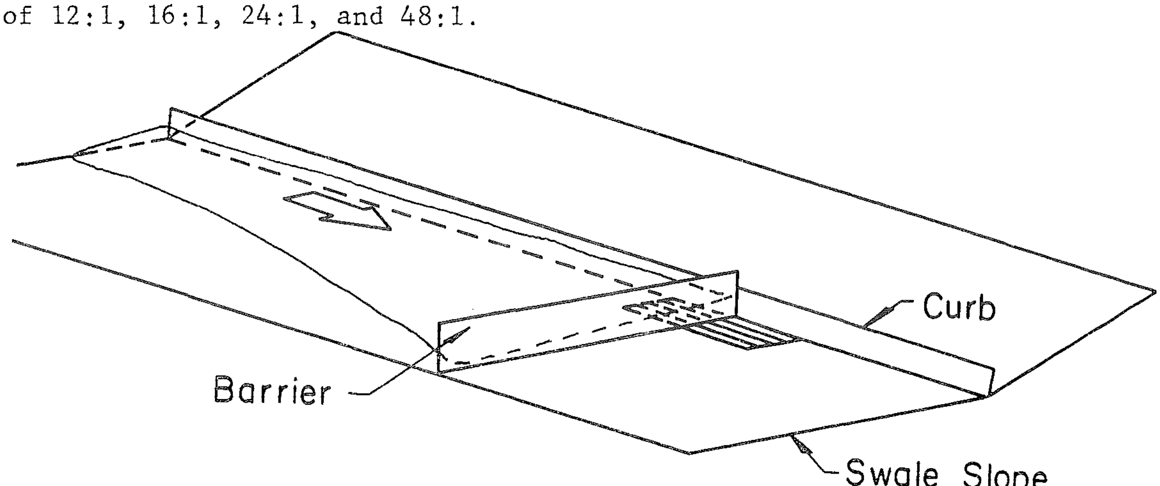

Fig. 5.1 Arrangement for Measurement of Sump Effect

The relation between the channel discharge in the prototype and in the model was not the same as it had been for all other tests which relation is shown in Section 2.4 as

$$\frac{Q_p}{Q_m} = 5.66, \tag{20a}$$

rather for the sump effect the relationship is doubled, or

$$\frac{Q_p}{Q_m} = 11.3 \tag{27}$$

The reason for the change is that the true capacity of an inlet, installed as shown in Fig. 5.1, is twice that recorded in this test inasmuch as a field installation has water flowing onto a grating from both longitudinal directions. Obviously then, in order to indicate the true capacity of a model inlet grating in a sump condition, the capacity, as determined in this study, must be doubled. This, of course, requires that the capacity of the prototype inlet grating be twice that indicated by means of Eq. (20a), which capacity is shown in Eq. (27).

Consequently in Table 5.1, Discharge and Spread for Different Back and Swale Slopes, the column headed "Discharge (cfs)" shows the capacity of a prototype grating that is receiving water from both directions.

The 8-ft spread of water on either side slope was not obtained because such data were not initially desired.

The efficiency column on each data sheet for sump tests, pages B-76 to B-87, is deleted because efficiency is of no significance in a sump test. Additionally, no carryover flow, Q_3, can be present in a sump test; this necessitates that Q_3 be replaced by Q_4, the latter being defined as spillage over the divisor. Such spillage occurred only during tests that involved the Type J Inlet.

5.2 Sump Effect of Type J Inlet

The data about the Type J Inlet for the sump effect are shown in Fig. 5.2 and are tabulated in Appendix B. A somewhat linear relationship exists between depth of water and discharge to a flow of 6 cfs; above that rate the water upstream from the inlet began to flow over the divisor which was 3-3/32 inches high. This is shown by dashed lines in Fig. 5.2. If the height of the divisor were increased somewhat, say 2 inches, the inlet would be able to take more runoff before flowing over the divisor and down onto the adjacent passing lane.

5.3 Sump Effect for Type 4-Ft Special Inlet

The data for the sump effect for the Type 4-Ft Special Inlet are given in Appendix B; they are graphed in Fig. 5.3 as depth of flow in the invert of the channel versus discharge in the channel.

The results appear as an approximate linear relationship between the two parameters. The inlet can take up to 14 cfs; that produces a depth that is over 1/2 ft in the invert. Such a flow would cause water to be spread over the entire width of pavement for a swale slope of 48:1. This condition is indicated by a nonsolid line on the graph.

5.4 Sump Effect for Type 6-Ft Special Inlet

The tests performed on the Type 6-Ft Special Inlet are recorded in Appendix B; the depth at the channel invert and the channel discharge are plotted in Fig. 5.4. A relationship as mentioned for the other inlets is also noted for the Type 6-Ft Special, that is, being somewhat linear. The maximal flow with greatest depth was observed on the steepest swale slope, which was 12:1.

For example, the capacity of this inlet was about 2 cfs more, at a depth of flow of 0.6 ft, than the capacity of the Type 4-Ft Special. This was particularly true for the very flat swale slope of 48:1. However, for the other swale slopes the greater capacity of the Type 6-Ft Special was only 1 cfs more at a depth of flow of 0.5 ft.

There does not appear to be a significant difference in capacity between the two Special Inlets; consequently either inlet can be used at the bottom of a vertical curve.

Type of Inlet	Back Slope	Swale Slope	Discharge (cfs)	Spread of Water on Swale Slope (ft)
6-Ft Special	1/8:1	48:1	9.88	>24
"	"	24:1	15.28	13.4
"	"	16:1	13.90	9.4
"	"	12:1	15.84	8.0
4-Ft Special	1/8:1	48:1	13.36	>24
"	"	24:1	14.28	14.6
"	"	16:1	14.82	11.2
"	"	12:1	14.82	8.8

Note:
(1) The discharge was the maximum for each test.
(2) Longitudinal slope was 0.2%.

Table 5.1 Discharge and Spread for Different Back and Swale Slopes

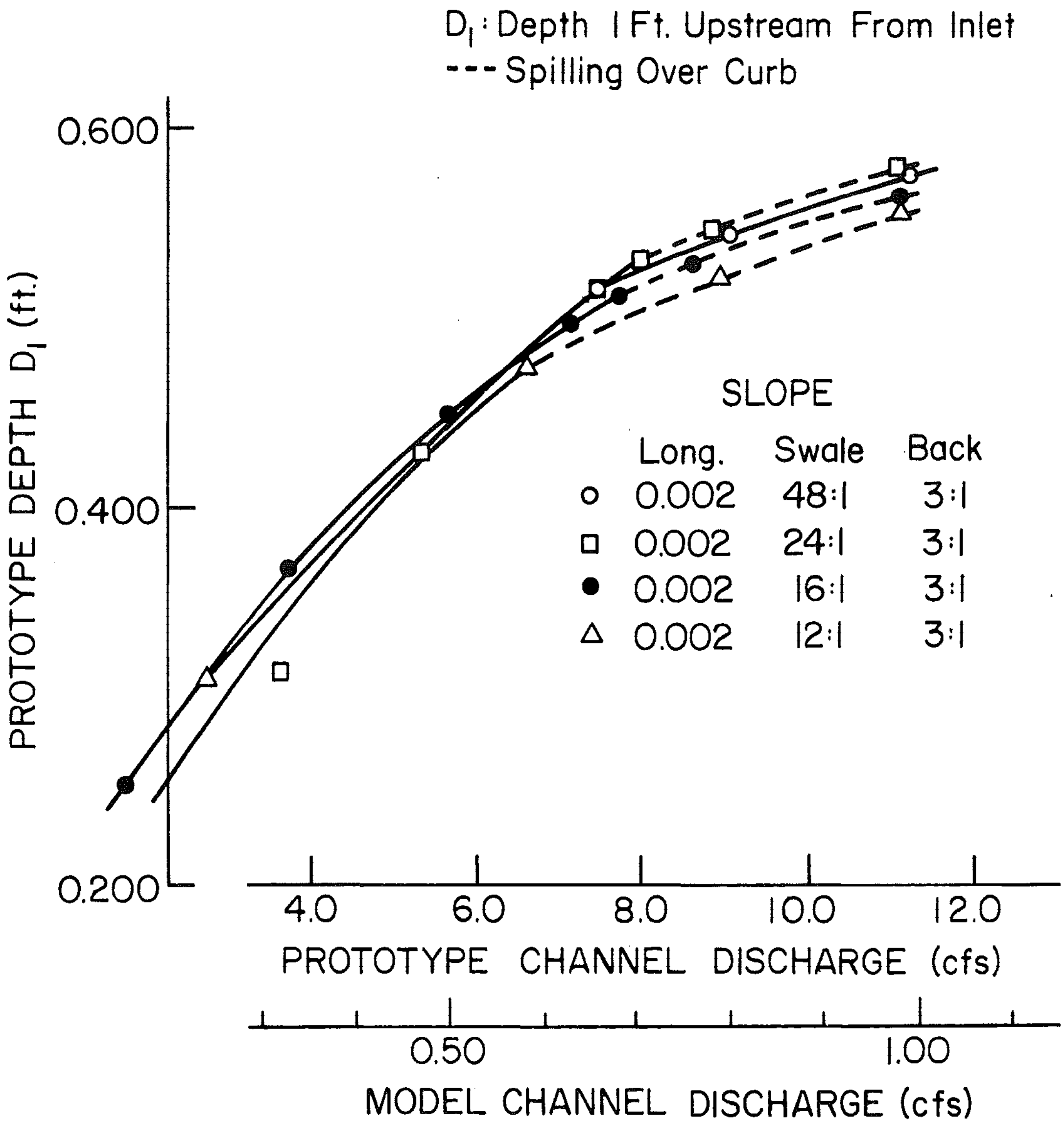

Fig. 5.2 Sump Effect for Type J Inlet

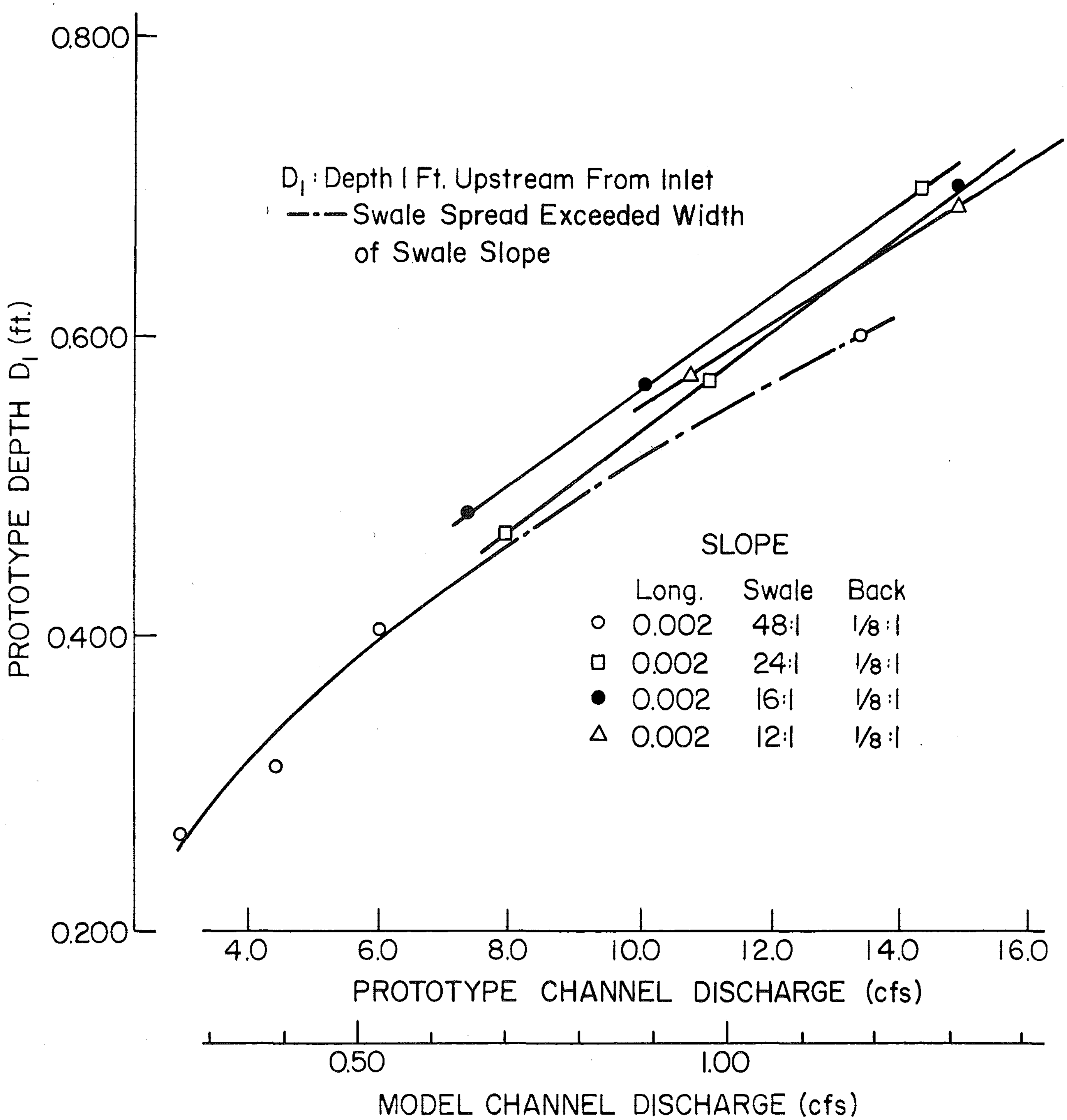

Fig. 5.3 Sump Effect for Type 4-Special Inlet

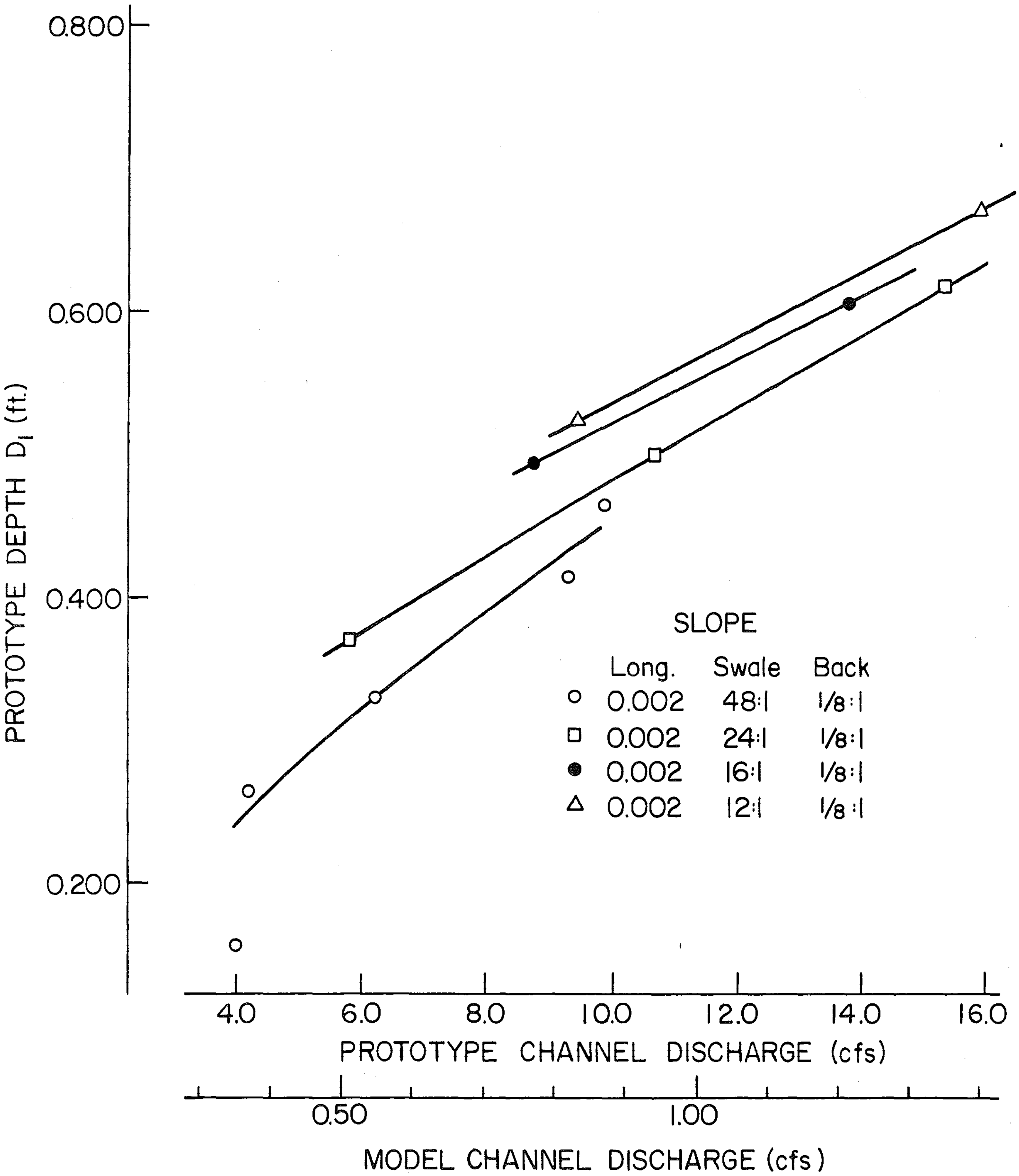

Fig. 5.4 Sump Effect for Type 6-Ft Special Inlet

6. DESIGN RECOMMENDATIONS

6.1 Introduction

This study was charged to determine the capacity and efficiency of drainage inlets being installed in paved channels along highways in Pennsylvania. The capacities of the inlets that were investigated are different from the design capacities used by the Pennsylvania Department of Transportation and shown in the Design Manual, Part 2: Highway Design, Commonwealth of Pennsylvania, Department of Transportation, page 2.12.20. The capacities are given as 5.50, 5.50, and 6.00 cfs for the Type J Inlet, the Type 4-Ft Special Inlet, and the Type 6-Ft Special Inlet, respectively.

6.2 Recommendation

The present investigation leads to a simplified listing of capacities for the above mentioned inlets, for a number of different conditions; the listing is tabulated in Appendix A, Section 2 wherein the capacity at an efficiency of 100% is indicated for four longitudinal slopes or grades, for four slopes of the swale, and for one back slope. The investigators feel that a design drainage efficiency of 100% (that is, all the water approaching an inlet being taken away by that inlet) should be used. This suggestion is made because all tests were done with water only, whereas in actual field situations debris will inevitably reduce the design efficiency. However, should a lower efficiency, say 90% or 75%, be desirable, a table similar to that in Section A.2 can be readily obtained from the efficiency curves of the drainage inlets which curves are given in Figures 4.1 to 4.12.

The tabulation in the Design Manual can now be changed so as to delete drainage inlet here discussed and their concomitant capacities and to insert the table of Section A.2.

In considering the positioning of drainage inlets, the design engineer is customarily provided with the following parameters: the class of highway, the alignment, and the topography of the site, which govern the grade or longitudinal slope as well as the back slope.

These three pieces of data namely the longitudinal slope, the swale slope, and the back slope, are sufficient to enter the proposed design table, which in turn gives the drainage inlet discharge at 100% efficiency.

7. ACKNOWLEDGMENTS

This research was sponsored by the Pennsylvania Department of Transportation in conjunction with the United States Federal Highway Administration. It was conducted in the Fritz Engineering Laboratory (Department of Civil Engineering) of Lehigh University at Bethlehem, Pennsylvania, by the following personnel of the Hydraulics and Sanitary Engineering Division: Dr. Arthur W. Brune, Project Director; Dr. Walter H. Graf, Associate Project Director; Dr. Stephen C. Ko, Research Associate; Mr. Erik Appel, Research Assistant; Mr. George M. Lee, Research Assistant; and Mr. Peter P. Yee, Research Assistant. Dr. Ko, Mr. Lee, and Mr. Yee are no longer with the project.

The Director of the Fritz Engineering Laboratory is Dr. Lynn S. Beedle. The Chairman of the Department of Civil Engineering is Dr. David A. VanHorn. The Director of the Office of Research is Professor George R. Jenkins.

The authors are indebted to Mr. Elias Dittbrenner who assisted in the work, to Miss Shirley Matlock who typed the manuscript, and to Mr. John M. Gera who prepared the drawings.

Recognition is here given to personnel of PennDOT who aided materially in the study, Mr. Melvin Bittenbender, PE, and especially Mr. Kenneth L. Heilman, PE, Research Coordinator, whose guidance was very helpful. Additionally, the authors offer their thanks to members of the FHWA, Mr. Donald M. Deuterman, Mr. Edison J. Foreman, but particularly to Dr. D. C. Woo, whose pertinent comments and remarks were particularly significant in accomplishing this work.

8. BIBLIOGRAPHY

1. Chow, V. T.
   OPEN-CHANNEL HYDRAULICS, McGraw-Hill Book Company, New York, New York (1959).

2. Graf, W. H.
   HYDRAULICS OF SEDIMENT TRANSPORT, McGraw-Hill Book Company, New York, New York (1971).

3. Guillou, J. C.
   THE USE AND EFFICIENCY OF SOME GUTTER INLET GRATES, University of Illinois, Engineering Exp. Sta., Bull. 450 (July 1959).

4. Henderson, F. M.
   OPEN CHANNEL FLOW, The Macmillan Company, New York, New York (1966).

5. Johns Hopkins University
   THE DESIGN OF STORM-WATER INLETS, Dept. of San. Engineering and Water Resources, Report of the Storm Drainage Research Committee, Baltimore, Maryland (June 1956).

6. Larson, C. L. and L. G. Straub
   GRATE INLETS FOR SURFACE DRAINAGE OF STREETS AND HIGHWAYS, University of Minnesota, St. Anthony Falls Hydraulic Laboratory, Bull. 2 (June 1949).

7. Morris, H. M.
   APPLIED HYDRAULICS IN ENGINEERING, The Ronald Press Company, New York, New York (1963).

8. Stevens, J. C., et al.
   HYDRAULIC MODELS, The Committee of the Hydraulics Division on Hydraulic Research, ASCE, Manual of Engineering Practice 25 (1942).

9. U. S. Army Corps of Engineers
   SURFACE DRAINAGE FACILITIES FOR AIRFIELDS, EM 1110-345-281, (1964).

10. Vennard, J. K.
    FLUID MECHANICS, 4th Edition, John Wiley and Sons, Incorporated, New York, New York (1966).

11. Yucel, O., et al.
    DEVELOPMENT OF IMPROVED DRAINAGE INLETS, PHASE 1: LITERATURE SURVEY, Lehigh University, Fritz Engineering Laboratory Report No. 364.2, (1969).

APPENDIX A IMPLEMENTATION STATEMENT

A.1 Preface

The present investigators propose the following changes in the Highway Design Manual of the Pennsylvania Department of Transportation as a consequence of the studies that have been performed.

A.2 Proposed Change in Highway Design Manual

In Chapter 12, DRAINAGE DESIGN, Capacity of Waterway Area, on page 2.12.20, delete the lines shown (4 foot special, 6 foot special, and J).

4. Depressed Medians

The width of water flowing in the median shall not exceed one half the total median width.

Inlets shall be provided to control the width of water in the median.

5. Structure Sections

See Part 4 of the Design Manual for specific instructions regarding superstructure drainage.

6. Inlets

When there is a change in pipe size in the inlet, the elevation for the top of pipes should be the same or the smaller pipe higher. A minimum drop of two inches should be provided in the inlet between the lowest inlet pipe invert elevation and the outlet pipe invert elevation.

Assumed inlet capacities shall be as follows:

Type	C.F.S.
A	0.50
B	0.50
C	3.50
D	3.50
E	3.50
F	3.50
4 foot	5.50
6 foot	6.00
~~4 foot special~~	~~5.50~~
~~6 foot special~~	~~6.00~~
~~J~~	~~5.50~~
H	5.50

Following the tabulation on page 2.12.20 insert the table of capacities for those inlets as here reproduced.

Slope (%)		Capacity (cfs)		
Longi-tudinal	Swale	Type J	Type 4-Ft Special	Type 6-Ft Special
1/2	12:1	0.68	1.47	2.66
"	16:1	0.57	1.47	1.47
"	24:1	0.48	0.30	0.94
"	48:1	0.22	0.17	0.22
2	12:1	0.57	2.77	4.02
"	16:1	0.42	2.07	3.68
"	24:1	0.30	1.78	2.35
"	48:1	0.30	0.60	0.68
4	12:1	0.48	3.40	4.08
"	16:1	0.37	2.55	2.89
"	24:1	0.37	1.19	1.55
"	48:1	0.30	0.42	0.66
8	12:1	1.34	2.41	2.74
"	16:1	1.08	1.95	1.75
"	24:1	0.57	1.22	1.19
"	48:1	0.22	0.45	0.74
Back Slope		3:1	1/8:1	1/8:1

Efficiency, η, is 100% for each condition, that is, no water overflows the inlet.

Capacity of Inlets--Type J, Type 4-Ft Special, and Type 6-Ft Special

On page 2.12.22 of the Manual for the lines which read:

Q = discharge capacity of the drainage facility (inlet, shoulder, swale, curb sections, etc.) with the least capacity;

insert the lines as follows:

Q = discharge capacity of the drainage facility (inlet, shoulder, swale, curb sections, etc.) with the least capacity. (For the capacities of inlets Type J, Type 4-Ft Special, and Type 6-Ft Special refer to the previous table.)

A.3 Commentary

The results of this study indicate that the capacities of the drainage inlets, designated as Type J, Type 4-Ft Special, and Type 6-Ft Special and installed in paved channels by the Pennsylvania Department of Transportation, as shown in its Highway Design Manual, are significantly larger than the capacities as determined during this investigation. This in turn more than justified the concern of the Pennsylvania Department of Transportation to have a testing program conducted on those inlets.

The capacities of these inlets depend upon three factors: the grade or longitudinal slope of the channel, the slope of the swale, and the back slope; the latter item, however, is not adjustable for either of the three inlets. The grade of the channel is not significant in causing a change in capacity for different grades; this was true for each inlet. In regard to the swale slope or paved portion of the channel, the steeper slope invariably results in a greater capacity for the inlet, but for the Type J inlet the difference is minor in terms of the amount of water entering the inlet. For the Special inlets the steeper swale slope enabled more water to enter the inlet which fact leads to those slopes having higher efficiencies.

An important point to consider is that the study was conducted with clear water; the water did not contain sand, soil particles, bits of leaves, or trash of any kind. It is therefore probable that a drainage inlet in the field might never reach the 100% efficiency owing to clogging of some openings in the grate.

A.4 Example

Given the following information:

1. Highway to be class 2.
2. Topography and alignment require a grade or a longitudinal slope of 2% and a swale slope of 24:1.
3. A Type 6-Ft Special Inlet is selected to be installed.

Solution:

4. Enter table of inlet capacities at a longitudinal slope of 2% and a swale slope of 24:1.
5. Read an inlet capacity of 2.35 cfs at an efficiency of 100%.
6. Insert 2.35 cfs for Q in the equation, $L = \frac{43,560\ Q}{C\ i\ W}$, PennDOT Highway Design Manual page 2.12.22, to determine the spacing, L, between adjacent inlets.

Note: If a Type 4-Ft Special Inlet had been selected, the discharge used in the above equation would have been 1.78 cfs, instead of 2.35 cfs.

APPENDIX B EXPERIMENTAL DATA

A complete set of sheets containing the experimental data pertaining to this Report is on file in the offices of

1. Pennsylvania Department of Transportation, Harrisburg, Pennsylvania;

2. Federal Highway Administration, Washington, DC; and

3. Department of Civil Engineering, Fritz Engineering Laboratory, Lehigh University, Bethlehem, Pennsylvania